

See discussions, stats, and author profiles for this publication at: <https://www.researchgate.net/publication/322866426>

# Individualized Model Predictive Control for the Artificial Pancreas: In Silico Evaluation of Closed-Loop Glucose Control

Article in IEEE control systems · February 2018

DOI: 10.1109/MCS.2017.2766314

CITATIONS

58

READS

1,115

4 authors, including:



Gian Paolo Incremona

Politecnico di Milano

66 PUBLICATIONS 1,078 CITATIONS

SEE PROFILE

Some of the authors of this publication are also working on these related projects:



Design of Collaborative Eco-Drive Control Algorithms for Train Networks [View project](#)



DRL and Robotics [View project](#)

# Individualized Model Predictive Control for Artificial Pancreas

in silico evaluation of closed-loop glucose control

Mirko Messori, Gian Paolo Incremona, Claudio Cobelli, and Lalo Magni

POC: M. Messori (mirko.messori01@ateneopv.it)

This is the final version of the paper accepted to be published on IEEE Control Systems Magazine

1 In each day of their life, patients affected by type 1 diabetes (T1D) must face the task of  
2 maintaining the blood glucose concentration, also called glycemia, within a safe range. T1D is  
a metabolic disorder characterized by a total insulin deficiency and, if not properly managed, it  
4 would result in chronic hyperglycemia, thus increasing the risk of severe long-term complications.  
Insulin is a hormone allowing utilization of glucose by body tissues and suppression of liver  
6 glucose production, and its shortage must be compensated with exogenous administration. The  
external insulin supply allows to avoid hyperglycemia, but, on the other hand, it can cause  
8 hypoglycemia if the amount of needed insulin is overestimated. Hypoglycemia is associated  
with short-term complications, which in severe cases can result in coma or death. In order to  
10 properly estimate the needed quantity of insulin, T1D patients normally rely on the conventional  
therapy, which is designed and continually updated by the physician, and consists of basal insulin  
12 (needed during fasting periods) and insulin boluses (needed to compensate the glucose rise due  
to meals).

14 Insulin can be delivered by injections or infusions. The latter is less invasive and requires a  
subcutaneous insulin pump, which continuously releases micro-boluses in the interstitial tissues  
16 of the patient and can be programmed with a patient-specific conventional therapy. Subcutaneous  
glucose sensing is also possible by continuous glucose monitor (CGM) devices, which are able  
18 to read the interstitial glucose concentration and inform the patient about glycemia levels and  
trends. The availability of subcutaneous insulin pumps and CGM has allowed the realization of  
20 the sensor augmented pump (SAP) therapy, which assists the patient in maintaining the glucose  
concentration within a safe range. However, with SAP, the patient still needs to decide how  
22 much insulin has to be infused by the pump on the basis of the CGM readings. The automation  
of the insulin infusion management can be reached with the artificial pancreas (AP), a system  
24 aimed at closed-loop glucose control.

The design of an AP dates from the seventies, when the first experiments were conducted with highly invasive intravenous systems [1]. In the following years, the AP systems have become progressively less invasive and portable and, thanks to the recent technological developments, the newer AP systems have become wearable and usable in free-living conditions. Since the subcutaneous route for a fully automatic blood glucose control was shown to be feasible [1], [2], the AP architecture includes a subcutaneous insulin pump for insulin delivery (actuator), a CGM for glucose sensing (sensor), and a standalone device aimed at the execution of the control algorithm (controller) [3]. This architecture, which relies on wireless connections among all the components, is the result of several clinical studies that were supported by the Juvenile Diabetes Research Foundation, the European Commission, and the National Institutes of Health [4]–[15].

The core of the AP is the control algorithm, which is in charge to estimate the proper quantity of insulin to infuse in the subcutaneous tissues during fasting, meal, and postprandial periods. Starting from 2008, several clinical trials have been performed by relying on a model predictive control (MPC) algorithm [16]–[20] in a hospital setting [21]–[26]. Subsequently, an improved MPC algorithm [27] based on the achieved clinical results has been adapted for outpatient studies [28]. The aim was to move the AP to free-living conditions for long periods and, in 2014, an AP system equipped with the MPC algorithm [27] has been used in the first randomized crossover outpatient clinical trial [15]. The AP was used for eight weeks during evening and night periods, paving the way for an extension study, completed in 2015, where the AP was continually used 24 hours per day for one month [29]. The results showed that MPC, of which a brief dissertation is presented in Sidebar 1, is a promising and feasible approach for AP. However, since different patients are characterized by different glucose-insulin dynamics, the control algorithm must be designed with robustness properties in order to make the closed-loop glucose control reliable and safe for each patient without compromising the desirable performance. Different dynamics are caused by the inter-subject variability, which reflects the different biological characteristics of each patient. Since an MPC algorithm determines the control actions on the basis of a model included in a cost function, patient-individualized glucose-insulin models are expected to further improve the glucose control performance. So far, the MPC used in the most recent clinical trials was synthesized on the basis of an average linear model [27]. The choice of using a linear model to describe the complex nonlinear glucose-insulin dynamics of diabetic patients is driven by the feasibility of the MPC implementation on a portable AP system [3], which is characterized by limited battery life and computational power. A similar approach, in which a compact model approximating the dynamics of the process under control was exploited to design the control law, was adopted in [30], in the context of type 2 diabetes. In this article, three customization techniques are considered to synthesize customized MPC based on patient-tailored linear models. The final aim is to show through closed-loop simulations that

customized MPC based on linear glucose-insulin models are able to improve the glucose control performance without losing the implementation feasibility on a portable AP device. The in silico results are presented and, in order to quantify the benefits of the customized MPC, a statistical comparison on the outcome metrics is performed vs. the non-customized MPC.

## Glucose-insulin models

The availability of a model describing the patient glucose-insulin dynamics is mandatory to synthesize an effective MPC. Indeed, one of the main ingredients needed for an MPC algorithm is a model describing the dynamics of the process under control (see Sidebar 1). In the context of AP, the reliability of the model glucose predictions are directly correlated to the efficacy of the controller, which commands the pump with the proper insulin to be infused as micro-boluses. A model able to predict the patient glycemia would be able to adjust the controller behavior in order to maintain the blood glucose concentration within the euglycemic range, which spans from 70 to 180 mg/dl, thus minimizing the risk of possible hyper- and hypoglycemia. However, methods used to directly measure the individual parameters of a T1D patient are invasive and expensive, making the identification of individualized glucose-insulin models a challenging task.

### UVA/Padova simulator

Several research groups have developed glucose-insulin models [31]–[33]. Of particular interest is the model developed by the Universities of Virginia and Padova (UVA/Padova) [34], which was included in the first simulator accepted by the Food and Drug Administration as a substitute to animal trials for pre-clinical testing of insulin therapies for T1D patients. The model included in the simulator is able to simulate the glucose-insulin dynamics of a specific person, and belongs to the class of compartmental models, of which a brief introduction is presented in Sidebar 2. The structure of the UVA/Padova simulator model is depicted in Figure 1. Different dynamics for different persons are simulated thanks to the availability of various sets of key metabolic parameters that describe the inter-subject variability of a generic population of T1D patients. Each set of parameters represents a “virtual subject” and has been identified from a large non-diabetic subject database where each subject underwent a triple tracer meal protocol that provided quasi-model-independent estimates of glucose and insulin fluxes [32]. The model was subsequently adapted to T1D by incorporating a model of subcutaneous insulin absorption and was shown to reliably describe the T1D literature data; three “virtual populations”, children, adolescents and adults, each composed of 100 subjects, were included in the simulator [34]. The UVA/Padova model has been then refined by improving the hypoglycemia glucose kinetics, by adding glucagon kinetics and secretion, and by refining the virtual subjects included in the

simulator [35] (see Figure 2). The clinical validity of the model was assessed on T1D data [36] and the circadian variability of insulin sensitivity and meal absorption parameters have been also included in the most recent version of the simulator [37], [38].

#### 4 Nonlinear time-variant model

The complete state-space representation of the nonlinear time-variant compartmental model depicted in Figure 1 is

$$\left\{ \begin{array}{l} \dot{x}_1(t) = -k_{gri} \cdot x_1(t) + d(t) , \\ \dot{x}_2(t) = k_{gri} \cdot x_1(t) - k_{empt}(x_1(t) + x_2(t)) \cdot x_2(t) , \\ \dot{x}_3(t) = -k_{abs}x_3(t) + k_{empt}(x_1(t) + x_2(t)) \cdot x_2(t) , \\ \dot{x}_4(t) = EGP(t) + Ra(t) - U_{ii}(t) - E(t) - k_1 \cdot x_4(t) + k_2 \cdot x_5(t) , \\ \dot{x}_5(t) = -U_{id}(t) + k_1 \cdot x_4(t) - k_2 \cdot x_5(t) , \\ \dot{x}_6(t) = -(m_2 + m_4) \cdot x_6(t) + m_1 \cdot x_{10}(t) + k_{a1} \cdot x_{11}(t) + k_{a2} \cdot x_{12}(t) , \\ \dot{x}_7(t) = -p_{2U} \cdot x_7(t) + p_{2U} \cdot \left( \frac{x_6(t)}{V_I} - I_b \right) , \\ \dot{x}_8(t) = -k_i \cdot x_8(t) + k_i \cdot \frac{x_6(t)}{V_I} , \\ \dot{x}_9(t) = -k_i \cdot x_9(t) + k_i \cdot x_8(t) , \\ \dot{x}_{10}(t) = -(m_1 + m_3(t)) \cdot x_{10}(t) + m_2 \cdot x_6(t) , \\ \dot{x}_{11}(t) = -(k_d + k_{a1}) \cdot x_{11}(t) + i(t) , \\ \dot{x}_{12}(t) = k_d \cdot x_{11}(t) - k_{a2} \cdot x_{12}(t) , \\ \dot{x}_{13}(t) = -k_{sc} \cdot x_{13}(t) + k_{sc} \cdot x_4(t) , \\ \dot{x}_{14}(t) = -n_G \cdot x_{14}(t) + SR_H(t) , \\ \dot{x}_{15}(t) = -k_H \cdot x_{15}(t) + k_H \cdot \max \{x_{14}(t) - H_b, 0\} , \\ \dot{x}_{16}(t) = \dot{S}R_H^s(t) , \end{array} \right. \quad (1)$$

where the meaning of all the states  $x_i(t)$ ,  $i = 1, \dots, 16$  are shown in Table 1. This model is included in the UVA/Padova simulator, and is characterized by the set of parameters listed in Table 2. Each set of parameter defines a virtual subject, and a set of virtual subjects defines a virtual population (Figure 2). The considered inputs are  $i(t)$  and  $d(t)$ , which represent the exogenous subcutaneous insulin infusion and the meal intake, respectively. The measurable output is the subcutaneous glucose concentration, which is calculated by dividing the glucose contained in the subcutaneous glucose compartment  $x_{13}$  by the compartment volume  $V_G$ . For more details about this model, the numerical values of the constant parameters, and the definition of the time-varying parameters, the reader is invited to refer to [34], [35] and references therein.

### Linearized average model

2 The UVA/Padova model is highly nonlinear and time-variant, and its incorporation in an  
MPC algorithm is computationally demanding, making the implementation on a portable AP  
4 device [3] practically unfeasible. Moreover, the key metabolic parameters associated with the  
nonlinear glucose-insulin dynamics of an individual are unknown, thus preventing the direct use  
6 of the UVA/Padova model for synthesizing an MPC suitable for clinical purposes.

Since the virtual population is thought to statistically represent the inter-subject variability  
8 of a generic population of T1D patients, an average time-invariant model representing the average  
dynamics of a diabetic patient can be computed by substituting all the time-varying parameters  
10 with their average values, and then by averaging all the available sets of key metabolic parameters  
(see Table 2). The average parameters are imposed in the model (1), which is subsequently  
12 linearized around a fictitious basal equilibrium corresponding to the basal glucose  $G_b$ , a steady  
state condition reached during fasting periods by infusing only basal insulin  $i_b$  [20]. Thus, by  
14 imposing  $i(t) = i_b(t)$  and  $d(t) = 0$ , the model reaches the fasting steady state equilibrium and  
is subsequently linearized to obtain a linear model defined as

$$\begin{cases} x(k+1) = Ax(k) + Bu(k) + Md(k) , \\ y(k) = Cx(k) , \end{cases} \quad (2)$$

16 where  $u(k)$  (pmol/ $t_s$ ) and  $d(k)$  (mg/ $t_s$ ) are two model inputs, which are associated with the  
variation of the subcutaneous insulin infusion with respect to the basal insulin, and with the  
18 meal intake, respectively; whereas  $y(k)$  (mg/dl) is the model output, which is the variation of  
the subcutaneous glucose concentration with respect to the fasting basal glucose  $G_b$ . Model (2) is  
20 written in state-space form, and is characterized by the state matrix  $A$ , a square matrix containing  
information about the relationships among all the model states. Several simulations have shown  
22 that the states  $x_{14}(t)$ ,  $x_{15}(t)$ , and  $x_{16}(t)$  of (1), which are associated with the glucagon system of  
Figure 1, can be neglected in the linear model without affecting the MPC control performance.  
24 Thus,  $A \in \mathbb{R}^{n \times n}$ , with  $n = 13$  denoting the total number of states of the linear model. Since the  
MPC algorithm running on the controller device is characterized by a sampling time  $t_s$ , model  
26 (2) is represented in discrete-time form. The average linearized model (2) can be considered  
to synthesize a non-individualized MPC with average glucose-insulin dynamics. This control  
28 approach, of which a detailed description can be found in [20], [27], has been utilized in several  
clinical trials performed in both adults [13], [15], [26], [28] and children [39].

### 30 Customized linear models

A non-individualized MPC based on an average model can be substantially penalized by  
32 the inter-subject variability affecting T1D patients. The latter can be handled with some forms

of models customization, thus defining models usable to synthesize MPC able to improve the glucose control performance. In this Section, three model customization techniques are presented, in particular two of them aim to identify individualized models able to reproduce patient-specific glucose-insulin dynamics. All the customized models presented in this section are characterized by the same inputs and output of the linearized average model (2).

### 6 *CR-based models*

The model customization approach described in [40] is based on subdividing the entire virtual population in subgroups. Each group is defined by considering the Insulin-To-Carbo Ratio (CR) parameter of each virtual subject. CR is a parameter that is part of the conventional therapy of the patient, and represents the nominal quantity of insulin bolus needed to compensate a meal through the relationship

$$i_B^{CR}(k) = \frac{d^g(k)}{CR(k)}, \quad (3)$$

where  $i_B^{CR}(k)$  (U) is the nominal insulin bolus that must be infused to compensate the estimated quantity of carbohydrates (CHO) included in the meal  $d^g(k)$  (g), and where  $CR(k)$  (g/U) is the CR value at time  $k$ , retrieved by considering the daily patient CR pattern. The subdivision presented in [40] defines four subgroups of the adult virtual population of the UVA/Padova simulator, each of which is composed of patients having low, medium-low, medium-high, and high insulin sensitivity (IS), respectively. The subgroups are defined as

$$\left\{ \begin{array}{ll} 1^{st} \text{ Group : } & \overline{CR} \leq 12 \quad 28 \text{ patients, low IS ,} \\ 2^{nd} \text{ Group : } & 12 < \overline{CR} \leq 15 \quad 21 \text{ patients, medium-low IS ,} \\ 3^{rd} \text{ Group : } & 15 < \overline{CR} \leq 19 \quad 21 \text{ patients, medium-high IS ,} \\ 4^{th} \text{ Group : } & \overline{CR} > 19 \quad 30 \text{ patients, high IS ,} \end{array} \right. \quad (4)$$

with  $\overline{CR}$  representing the average value of the daily CR pattern, and where 12, 15, and 19 are the integer approximations of the 25-th, 50-th, and 75-th percentiles associated with the CR distribution of the adult virtual population (see Figure 3). For each subgroup, an average model is computed and then linearized around the basal equilibrium, thus obtaining four linear models having the form of (2), which can be used to synthesize an MPC. The customization consists in synthesizing the MPC by selecting the most appropriate model for a generic patient by considering his/her  $\overline{CR}$  value, which is used to determine to which group the patient belongs.

### 26 *Nonparametric models*

The CR-based customization approach defines a set of models that can be used to synthesize a customized MPC based on the patient estimated insulin sensitivity. However,

further improvements are expected in closed-loop glucose control with MPC based on patient-  
 tailored models that incorporate patient-specific glucose-insulin dynamics. The nonparametric  
 (NP) approach described in [41] belongs to the class of black-box identification and can be used  
 to identify patient-specific glucose-insulin models by relying on historical insulin administrations  
 and meal intakes (inputs), and CGM measurements (output). Given a set of historical input-output  
 data associated with a specific patient, the NP approach identifies a one-step ahead predictor  
 that is subsequently converted in a state space model obtained through a minimal realization of  
 a given dimension. The identification process is performed through a kernel-based regression in  
 which the stable spline kernel introduced in [42] is considered. The final result is the identification  
 of a linear time-invariant model having the form

$$y(t) = \sum_{k=1}^{p_l} q_u(k)u(t-k) + \sum_{k=1}^{p_l} q_d(k)d(t-k) + \sum_{k=0}^{p_l} w(k)e(t-k), \quad (5)$$

where  $e(k)$  is a white Gaussian noise signal representing the uncertainties affecting the model  
 and where the Z-transforms of  $q_u(k)$ ,  $q_d(k)$ , and  $w(k)$  are given by

$$Q_u(z) = \frac{\sum_{k=1}^{p_l} g_1(k)z^{-k}}{1 - \sum_{k=1}^{p_l} f(k)z^{-k}}, \quad Q_d(z) = \frac{\sum_{k=1}^{p_l} g_2(k)z^{-k}}{1 - \sum_{k=1}^{p_l} f(k)z^{-k}}, \quad W(z) = \frac{1}{1 - \sum_{k=1}^{p_l} f(k)z^{-k}}, \quad (6)$$

with  $p_l$  denoting a tunable parameter. The quantities  $g_1$ ,  $g_2$ , and  $f$  represent the impulse responses  
 related to insulin, meals, and to the Gaussian noise, and are identified through the kernel-based  
 regression process. Thus, the individualized MPC is synthesized by relying on the following  
 state-space augmented model achieved through minimal realization:

$$\begin{cases} x_{NP}(k+1) = A_{NP}x_{NP}(k) + B_{NP}u(k) + M_{NP}d(k) + W_{NP_x}e(k), \\ y(k) = C_{NP}x_{NP}(k) + W_{NP_y}e(k), \end{cases} \quad (7)$$

where  $x_{NP}$  is a vector of maximum dimension  $p_l$  containing the internal states,  $A_{NP}$ ,  $B_{NP}$ ,  $C_{NP}$ ,  
 $M_{NP}$  are matrices of proper dimensions,  $W_{NP_x}$  is a column vector (with maximum dimension  
 $p_l$ ), and  $W_{NP_y}$  is a scalar value.

### 20 *Constrained optimization models*

The NP approach identifies linear models with an unknown internal structure, since it is  
 a black-box identification technique. Indeed, there is no control on the achievable number of  
 internal states, which can be only limited to  $p_l$ , a parameter that however must be set “large  
 enough” to capture the essential dynamics of the patient. Having a linear model with a large  
 number of internal states could be an issue for the MPC algorithm implementation, which must  
 reside on a standalone device with limited computational power and memory. In order to identify



a linear model having a fixed parametric structure, the grey-box identification approach based on the constrained optimization (CO) process described in [41] is considered. By considering the linearization of the UVA/Padova model (1) around the basal equilibrium point, the parametric model structure

$$\begin{cases} x_{CO}(k+1) = A_{CO}x_{CO}(k) + B_{CO}u(k) + M_{CO}d(k) , \\ y(k) = C_{CO}x_{CO}(k) , \end{cases} \quad (8)$$

having the same form of (2) is postulated, where  $x_{CO}$  is a vector containing the  $n = 13$  model states, and where the matrices  $A_{CO} \in \mathbb{R}^{n \times n}$ ,  $B_{CO} \in \mathbb{R}^{n \times 1}$ ,  $C_{CO} \in \mathbb{R}^{1 \times n}$ , and  $M_{CO} \in \mathbb{R}^{n \times 1}$  are identified through the solution of the constrained optimization problem described in [41]. The identification is performed by relying on historical input-output data associated with the patient.

Unlike with the NP approach, the CGM subcutaneous glucose measurements (output data) need to be pre-filtered prior to be considered for identification. The pre-filtering is used to reduce the noise component affecting the CGM measurements, which could significantly reduce the identifiability of the patient glucose-insulin dynamics. The pre-filtering process can be performed with several techniques. A simple technique considers the moving average filter

$$y_{MA}(k) = \frac{\sum_{j=0}^{N_{MA}-1} CGM(k-j)}{N_{MA}} ,$$

where  $y_{MA}$  (mg/dl) is the pre-filtered output data used in the identification process,  $CGM(k)$  is the measured subcutaneous glucose by the CGM at time  $k$ , and  $N_{MA}$  is the considered moving average length. Pre-filtering techniques that are more specific for CGM measurements can also be considered, like the retrofitting process described in [43]. Despite the need of pre-filtering, a substantial advantage of the CO approach with respect to the NP is represented by the fixed parametric structure of the identified model, which results in a fixed implementation complexity of the MPC algorithm for any patient. Moreover, it has been shown that the CO approach is able to capture the glucose-insulin dynamics of the patient by relying on shorter identification data-sets [41], which are more easily realizable in a real life scenario, where the patient would be enrolled in a clinical study to produce historical input-output data for identification purposes.

## Closed-loop glucose control

The presented identification approaches aim to identify individualized glucose-insulin models to be included in the MPC algorithm, thus defining an individualized control law for the AP system. Preliminary closed-loop results were obtained in silico through customized MPC with CR-based models [40], and through individualized MPC based on nonparametric [44] models.

In this article, these closed-loop results are refined and compared with the results achieved in closed-loop through the individualized MPC based on the CO models.

A schematic AP representation is depicted in Figure 4. The MPC algorithm is the core of the AP, and is in charge to properly command the insulin pump on the basis of CGM subcutaneous glucose readings. Of particular interest are the meals, which are considered as substantial disturbances affecting the glucose concentration and are handled through the meal announcement, a feedforward action controlled by the patient [20]. The MPC algorithm can also use information contained in the conventional therapy, which is adapted to the patient and continually updated by the physician.

## Conventional Therapy

Diabetic patients can rely on the conventional therapy, which is adapted by the physician to the patient and is composed of the basal insulin, which is the insulin needed to maintain the patient glycemia to a target during fasting periods, and the insulin bolus, which is the insulin needed to compensate the increase in glycemia due to a meal. The insulin suggested by the conventional therapy is defined as

$$i(k) = i_B(k) + i_b^U(k) ,$$

where  $i_B(k)$  (U) is the insulin bolus associated with the meal taken at time  $k$ , and  $i_b^U(k)$  (U) is the patient basal insulin, usually represented as a piecewise constant function. The insulin bolus  $i_B$  is strictly correlated to the amount of CHO that the patient assumes with the meal, and can be represented as insulin spikes that are significantly higher with respect to basal. The insulin bolus calculation is defined as

$$i_B(k) = i_B^{CR}(k) + \frac{BG(k) - y_{CF}}{CF(k)} - i_{IOB}^h(k) , \quad (9)$$

where the CR-based insulin bolus  $i_B^{CR}(k)$  defined in (3) is refined with the addition of two terms. The first term uses one of the parameters included in the conventional therapy, the correction factor (CF), to adjust the insulin bolus on the basis of the difference between the blood glucose (BG) and a target glucose concentration  $y_{CF}$  (mg/dl). BG is usually measured through a fingerstick device, which measures the blood glucose concentration in a drop of blood. The second term reduces the insulin bolus on the basis of the insulin on board (IOB)  $i_{IOB}^h(k)$  (U), which is the estimated residual insulin that has still effect. IOB is estimated through insulin

decay curves [45]

$$\begin{cases} i_{IOB}^h(k) = 100 \cdot \left( 1 - k_a^h \frac{f_{IOB}^h(k)}{k_{den}^h} \right), \\ f_{IOB}^h(k) = \frac{a_3}{a_1 \cdot (a_1 - a_2)} \left( e^{\frac{-a_1 \cdot k}{k_a^h}} - 1 \right) - \frac{a_3}{a_2 \cdot (a_1 - a_2)} \left( e^{\frac{-a_2 \cdot k}{k_a^h}} - 1 \right), \end{cases} \quad (10)$$

2 where all the constants are properly chosen on the basis of the time of decay  $h$ . The time course  
of the insulin decay curves for different values of decay is depicted in Figure 5. In the case of  
4 adult patients, the decay curve having  $h = 4$  hours is usually considered to estimate the IOB.

### MPC algorithm definition

6 One of the aspects that makes the design of an AP system challenging is the presence of  
unavoidable delays and inaccuracies in both subcutaneous glucose sensing and insulin delivery.  
8 Coping with these issues is particularly difficult when a system disturbance like a meal occurs  
and triggers a rapid glucose rise that is substantially faster with respect to the time needed  
10 in particular for insulin absorption. In presence of inherent delays, any attempt to speedup  
the responsiveness of the closed-loop system may result in an unstable system behavior and  
12 oscillations. A good controller should consider a relatively slow response, however, a too slow  
control law could not be able to properly attenuate the postprandial glucose peaks. Thus, the AP  
14 system must be designed with a controller able to deal with a trade-off between slow and fast  
regulation [5]. A slow regulation must be considered during quasi-steady state conditions, like  
16 overnight, whereas a fast regulation is useful during postprandial periods, where timely insulin  
infusions are needed.

18 An MPC for AP is a model-based control approach that uses a model to predict the patient  
glucose-insulin dynamics. The subcutaneous insulin pump is properly commanded with insulin  
20 infusions based on the predicted patient glycemia within a predefined prediction horizon. As  
shown in Figure 4, the MPC algorithm is enriched with information contained in the patient's  
22 conventional therapy and with the meal announcement, which is a feedforward action activated  
by the patient at meal times. Meal announcement is used to "inform" the controller that the  
24 glycemia is expected to rise rapidly due to a meal, thus requiring prompt insulin delivery. This  
information is provided to the controller by the glucose prediction computed through the built-in  
26 linear model having the form of (2), (7), or (8), which is triggered by the meal announced in the  
meal input  $d$ . The presence of a feedforward action makes the AP system not fully automated.  
28 However, meal announcement must be considered as additional knowledge that is available to  
the patient and that should be exploited to improve the postprandial glucose control. In case of  
30 missing meal announcement, in spite of an unavoidable worsening of the control performance,

the AP must remain able to operate safely.

## 2 Closed-loop scheme

The AP closed-loop scheme is shown in Figure 6, where the blue blocks represent the MPC and the patient, yellow blocks represent the hardware, and the green block represents the conventional therapy used to compute the nominal insulin boluses through formula (9), which is used in the meal announcement. This scheme is defined on top of the conventional therapy in the sense that the MPC is in charge to suggest insulin variations with respect to that therapy. Indeed, during fasting periods, the MPC suggests insulin variations with respect to the patient basal insulin  $i_b$ . On the other hand, when a meal is announced, the controller receives information about the nominal insulin bolus  $i_B$ , and is in charge to eventually modify this value based on the estimated state of the patient.

## 12 Controller cost function and calibration

The MPC insulin suggestions are driven by the quadratic cost function

$$J(\hat{x}(k|k), u(\cdot), k) = \sum_{i=0}^{N-1} (q(y(k+i) - y_{sp}(k+i) + G_b(k+i))^2 + (u(k+i) - u^0(k+i))^2) + \|x(k+N)\|_P^2, \quad (11)$$

such that

$$\begin{aligned} x(k) &= \hat{x}(k|k), \\ y(k) &= C\hat{x}(k|k), \\ x(k+i+1) &= Ax(k+i) + Bu(k+i) + Md(k+i), \\ y(k+i+1) &= Cx(k+i+1), \\ u^0(k+i) &= i(k+i) - i_b(k+i), \end{aligned}$$

where  $\hat{x}(k|k)$  is the state estimated through the Kalman filter described in [27] at time  $k$ ,  $u^0$  is the variation of the insulin suggested by the conventional therapy with respect to the basal insulin  $i_b$ ,  $y_{sp}$  (mg/dl) is the desired glucose set-point,  $N$  is the prediction horizon,  $q > 0$  is a tunable parameter, and  $P$  is the unique nonnegative solution of the discrete time Riccati equation (S5). The matrices  $A$ ,  $B$ ,  $C$ , and  $M$ , define the linear glucose-insulin model used to predict the patient glycemia within the horizon  $N$ . Any linear model having the form (2) can be included in the cost function or, alternatively, the identified models (7) or (8) can be considered, thus defining an individualized controller.

The cost to be minimized includes the glucose set-point and the conventional therapy in the terms  $y_{sp}$  and  $u^0$ , respectively. The insulin suggestion is calculated by computing the optimal

tradeoff between the glucose error with respect to the set-point and the insulin variations with respect to the conventional therapy. The tradeoff is defined through the parameter  $q$ . Higher  $q$  values are associated with a higher cost to the glucose variations, thus resulting in a more aggressive controller that strives for maintaining the glycemia to the set-point. On the other hand, lower  $q$  values are associated with a higher cost to the insulin variations with respect to the conventional therapy, resulting in a more conservative controller.

The  $q$  value must be set on the basis of the estimated insulin sensitivity of the patient. Patients that are more insulin-sensitive require a more conservative controller, whereas patients characterized by elevated insulin resistance require more aggressive insulin administrations. The tuning of  $q$  is handled through a calibration procedure that is performed in simulation by considering a trial and error approach driven by the performance index

$$J_q(q) = \sqrt{X_{CVGA}^2 + Y_{CVGA}^2} + k_1^C \cdot (\log_{10}(q) - k_2^C)^2, \quad (12)$$

where  $X_{CVGA}$  and  $Y_{CVGA}$  are the coordinates achieved in simulation in the control variability grid analysis (CVGA) defined in [20], [46], and  $k_1^C$  and  $k_2^C$  are tunable parameters. The CVGA coordinates are obtained by simulating a predefined calibration scenario and the process is repeated until the minimum cost  $J_q$  is found. The flow chart representing the calibration procedure is shown in Figure 7. A linear model for control synthesis is used to synthesize the MPC that is used to simulate the closed-loop control on a model for control testing. At the end of each simulation, the performance index (12) is evaluated and the process is repeated until the decrease of the performance index becomes negligible, thus resulting in the calibrated  $q$  value

$$\hat{q} = \min\{\max\{\arg \min_q \{J_q(q)\}, \bar{q}_l\}, \bar{q}_h\},$$

where  $\bar{q}_l$  and  $\bar{q}_h$  are minimum and maximum safety thresholds, respectively.

In case of individualized models, the model for control testing is the same model used for control synthesis. This procedure is feasible in a real scenario, where the identified model would be used for the trial and error approach, and the real patient would be equipped with the controller including the resulting calibrated  $\hat{q}$ . In case of MPC based on non-individualized models, the calibration procedure is repeated for each virtual subject, which is characterized by the model (1), considered as the model for control testing. The regression model

$$\hat{q}(BW, CR) = e^{r_1 \cdot BW + r_2 \cdot CR + r_{int}}$$

is then used to adapt the  $q$  value to each patient on the basis of his/her CR and body weight (BW). As described in [27], the parameters  $r_1$ ,  $r_2$ , and  $r_{int}$  were obtained by relying on 100 calibrated  $\hat{q}$  associated with the entire adult virtual population of the UVA/Padova simulator.

## Simulation results

2 The MPC considered in simulation is entirely defined in [27]. MPC is equipped with  
properly defined insulin constraints and is driven by the cost function (11). In order to have an  
4 estimation of the MPC behavior in a real scenario, the simulations were performed on the 100  
non-linear time-variant adult virtual subjects of the UVA/Padova simulator [35]. Furthermore, in  
6 order to test the controller safety and robustness, the insulin sensitivity of each virtual subject  
was randomly varied by a  $\pm 25\%$  factor and the controller was blind to these variations.

8 The simulation scenario is shown in Figure 8 and includes five meals, of which the first  
is compensated in open-loop (through the conventional therapy), while the remaining meals are  
10 compensated through the MPC. The simulation scenario starts at 6:00 and lasts 34 hours, and  
the loop is closed at 8:00. Note that the loop is closed within the postprandial period of the  
12 open-loop compensated meal, increasing the variability associated with the closed-loop starting  
conditions. Meal amounts are 50 g CHO for the first breakfast, 60 g CHO for the second one,  
14 60 for the two lunches, and 80 g CHO for the dinner. Postprandial periods are defined as 4-hour  
time intervals starting from each meal time. Night period starts at 23:00 and lasts eight hours.

16 The glucose control performance is evaluated through standard indices in evaluating AP  
clinical trials [47]. The considered metrics are the following: average glucose (A), glucose  
18 standard deviation (SD), glucose coefficient of variation (CV), time in target or percentage  
of time spent within 70-180 mg/dl (Tt), time in tight target or percentage of time spent within  
20 70-140 mg/dl (Ttt), time above target or percentage of time spent above 180 mg/dl (Ta), time  
below target or percentage of time spent below 70 mg/dl (Tb), number of hypo-treatments (#ht),  
22 and number of patients with at least one hypo-treatment (# patients with ht). A hypo-treatment  
consists of 16 g CHO that are administered in case the patient glycemia falls below 65 mg/dl. This  
24 process is automatically performed in the simulation environment with a constraint that imposes  
a time gap of at least 30 minutes between two consecutive hypo-treatments. In addition, insulin  
26 metrics are also included in terms of daily insulin needs (measured in insulin units U), and daily  
insulin needs normalized by the patient weight (U/kg).

Table 3 shows the outcome indices achieved through the linearized non-individualized  
MPC (L-MPC), through the customized MPC based on the CR-based models (CR-MPC), and  
through the individualized MPCs synthesized by considering the nonparametric models (NP-  
MPC), and the models identified through constrained optimization (CO-MPC). Both NP-MPC  
and CO-MPC were synthesized based on individualized models identified from historical input-  
output data generated in silico by following the identification scenarios described in [41]. Each  
index is evaluated during the overall scenario (O), during the night (N), and within the closed-

loop postprandial periods (PP). Non-normal data are shown as median (25-th percentile, 75-th percentile), whereas normal data are shown as mean (standard deviation). Given that all the Tb percentiles of Table 3 are equal to zero, in order to perform a quantitative comparison, Table 4 shows the Tb indices in terms of mean (standard deviation). Statistical comparisons are performed between L-MPC and the customized MPCs with the following significance levels:

$$\text{p-value } (p) \text{ significance level} = \begin{cases} \dagger & p < 0.05 , \\ \dagger\dagger & p < 0.01 , \\ \dagger\dagger\dagger & p < 0.001 , \end{cases}$$

where  $p$  is evaluated with the paired t-test for normally distributed data and with the Wilcoxon signed-rank test otherwise. The test of normality is performed through the Lilliefors test.

From now on, for easy reading, CR-MPC, NP-MPC, and CO-MPC will be referred as individualized MPCs.

The individualized MPCs significantly reduced the average glucose. The reduction is more noticeable with NP-MPC and CO-MPC, which are synthesized on patient-individualized glucose-insulin models. Although the achieved time in target is numerically similar with all the considered controllers, the individualized MPCs significantly increased the time in tight target and reduced the time above target without increasing the time below target. The reduction of hyperglycemia was also significant with the exception of CO-MPC, which used a significantly lower amount of insulin with respect to the other controllers and encountered only two hypo-treatments in only one patient within the entire adult virtual population. Thus, it is possible to conclude that the individualized MPCs are able to maintain more steady the glucose concentration without significantly increasing the risk of hyper- or hypoglycemia.

Glucose control is particularly challenging within the postprandial periods, where the rapid increase of glucose induced by a meal must be promptly compensated by taking into account the risk of induced postprandial hypoglycemia. As shown in Figure 9, the postprandial glucose compensation is slightly improved with CR-MPC with respect to L-MPC since the glucose peaks are lower and the glucose decrease is faster. However, both these controllers are characterized by a conservative behavior at the end of each postprandial period, where the glycemia decrease is systematically slowed down before reaching the glucose set-point (120 mg/dl). This conservative compensation was introduced to minimize the risk of postprandial hypoglycemia, which is caused by insulin overestimation for meal compensation and would require a hypo-treatment to restore the proper glucose concentration. Thanks to the availability of patient-individualized models, this behavior is no longer noticeable in NP-MPC and CO-MPC, which can rely on more effective glucose predictions. Thus, both the controllers based on patient-individualized models are able to compensate faster the postprandial glycemia and to reach the glucose set-point without slowing

down the glycemia decrease for safety purposes. In particular, CO-MPC is able to quickly  
2 compensate the postprandial glycemia without creating glucose undershoots before reaching the  
set-point. This behavior is evident in Figure 9, where the shadowed region representing the  
4 glucose variability of CO-MPC is narrower with respect to NP-MPC.

The faster glucose compensation of NP-MPC and CO-MPC significantly increases the  
6 postprandial SD and CV, as shown in Table 3, consequently increasing the same indices in  
the overall scenario. However, as shown in the CVGA of Figure 10, this does not translate  
8 into a worsening of the overall control performance. Each point in the CVGA represents the  
combination of the minimum and the maximum glycemia reached by each patient during a  
10 simulation. A point is present for each patient for each one of the four considered MPCs, thus  
resulting in 400 points. Although the number of points in the A region is reduced with NP-MPC  
12 and CO-MPC, their scatter plots are within the A and B regions, denoting that the overall glucose  
control performance is not compromised. Moreover, CO-MPC results in 96 points included in  
14 the A and B regions and no points in the D region, thus achieving the best performance in terms  
of CVGA.

## 16 Conclusion

Although the continuous efforts devoted to the AP development in the last decades,  
18 nowadays an AP system is not yet available in the market. One of the major issues regards  
the inter-subject variability affecting T1D patients, which makes the definition of a single  
20 controller suitable for any patient practically impossible. Moreover, a state of the art non-invasive  
and portable AP system is composed of subcutaneous hardware components, and the control  
22 algorithm must be properly designed to reside on a standalone device with limited battery life  
and computational power. These characteristics make the design of a safe and effective AP  
24 system even more challenging due to the inherent delays affecting the subcutaneous insulin  
delivery route, and due to the tradeoff between control performance and computational power  
26 expenditure.

Thanks to its capability of dealing with inherent delays of the process under control, the  
28 MPC is one of the most promising control approaches in the context of AP. However, the  
achievable control performance is strictly related to the prediction capabilities of the model  
30 included in the controller, which in general can be highly nonlinear. The currently used MPC in  
clinical experiments relies on a linear average glucose-insulin model designed to represent the  
32 average dynamics of a subject with diabetes. This non-individualized MPC is not designed to  
cope with patient-specific dynamics, but is designed to be non-computationally demanding and  
34 robust enough to result in a safe and effective control law.



2 The introduction of patient-tailored glucose-insulin linear models opens the way for  
3 designing individualized MPCs capable of significantly improving the achievable glucose  
4 control performance and enhancing the AP system safety and efficacy without increasing the  
5 computational complexity of the control algorithm. The closed-loop simulations have shown that  
6 the individualized MPCs are able to cope with the inter-subject variability, and are particularly  
7 effective within the postprandial periods, where the patient glycemia is substantially perturbed  
8 and the controller needs to react promptly to compensate the glucose rise without inducing  
9 postprandial hypoglycemia.

10 The proposed individualization approaches are not thought to deal with intra-subject  
11 variability (which represents the variability characterizing a specific patient over time), and future  
12 investigation both in silico and in vivo will need to take this variability into account. However,  
13 in order to achieve preliminary clinical results on the safety and feasibility of the proposed  
14 identification approaches, future works will consider the identification of individualized glucose-  
15 insulin models from clinical data of patients with T1D. Clinical studies will have to be designed  
16 to achieve sufficiently perturbed clinical data aimed at models identification. Indeed, as described  
17 in [41], one of the major issues associated with models individualization is the glucose-insulin  
18 dynamics identifiability. The CO approach is preferable with respect to the NP, since it identifies  
19 linear compartmental models having a fixed structure, and requires a shorter identification data-  
20 set that would be more easily realizable in a real scenario. Thus, individualized MPCs usable in  
21 clinical trials will be synthesized, having the potential of further improving the clinical results  
22 and making a significant step towards in the design of an AP device suitable for the market.

## 22 **References**

- 23 [1] C. Cobelli, E. Renard, and B. P. Kovatchev, “Artificial pancreas: past, present, future,”  
24 *Diabetes*, vol. 60, no. 11, pp. 2672–2682, 2011.
- 25 [2] G. M. Steil, K. Rebrin, C. Darwin, F. Hariri, and M. F. Saad, “Feasibility of automating  
26 insulin delivery for the treatment of type 1 diabetes,” *Diabetes*, vol. 55, no. 12, pp. 3344–  
3350, 2006.
- 27 [3] M. Messori, C. Cobelli, and L. Magni, “Artificial pancreas: from in-silico to in-vivo,” in  
28 *IFAC 9th International Symposium on Advanced Control of Chemical Processes*, Whistler,  
29 British Columbia, Canada, June 7–10 2015, pp. 1301–1309.
- 30 [4] B. W. Bequette, “Challenges and recent progress in the development of a closed-loop  
31 artificial pancreas,” *Annu Rev Control*, vol. 36, no. 2, pp. 255–266, 2012.
- 32 [5] C. Cobelli, C. Dalla Man, G. Sparacino, L. Magni, G. De Nicolao, and B. P. Kovatchev,  
33 “Diabetes: models, signals, and control,” *IEEE Rev. Biomed. Eng.*, vol. 2, pp. 54–96, 2009.  
34

- [6] F. H. El-Khatib, S. J. Russell, D. M. Nathan, R. G. Sutherlin, and E. R. Damiano, “A bihormonal closed-loop artificial pancreas for type 1 diabetes,” *Sci Transl Med*, vol. 2, no. 27, p. 27ra27, 2010.
- [7] R. Hovorka, J. M. Allen, D. Elleri, L. J. Chassin, J. Harris, D. Xing, C. Kollman, T. Hovorka, A. M. F. Larsen, M. Nodale, A. De Palma, M. E. Wilinska, C. L. Acerini, and D. B. Dunger, “Manual closed-loop insulin delivery in children and adolescent with type 1 diabetes: a phase 2 randomised crossover trial,” *The Lancet*, vol. 375, no. 9716, pp. 743–751, 2010.
- [8] S. A. Weinzimer, G. M. Steil, K. L. Swan, J. Dziura, N. Kurtz, and W. V. Tamborlane, “Fully-automated closed-loop insulin delivery versus semi-automated hybrid control in pediatric patients with type 1 diabetes using an artificial pancreas,” *Diabetes Care*, vol. 31, no. 5, pp. 934–939, 2008.
- [9] R. Hovorka, “Closed-loop insulin delivery: from bench to clinical practice,” *Nat. Rev. Endocrinol.*, vol. 7, no. 7, pp. 385–395, 2011.
- [10] M. Breton, A. Farret, D. Bruttomesso, S. Anderson, L. Magni, S. Patek, C. Dalla Man, J. Place, S. Demartini, S. Del Favero, C. Toffanin, C. Hughes-Karvetski, E. Dassau, H. Zisser, F. J. Doyle III, G. De Nicolao, A. Avogaro, C. Cobelli, E. Renard, and B. Kovatchev, on behalf of The International Artificial Pancreas (iAP) Study Group, “Fully integrated artificial pancreas in type 1 diabetes: modular closed-loop glucose control maintains near normoglycemia,” *Diabetes*, vol. 61, no. 9, pp. 2230–2237, 2012.
- [11] F. J. Doyle, L. M. Huyett, J. B. Lee, H. C. Zisser, and E. Dassau, “Closed-loop artificial pancreas systems: engineering the algorithms,” *Diabetes Care*, vol. 37, no. 5, pp. 1191–1197, 2014.
- [12] S. J. Russell, F. H. El-Khatib, M. Sinha, K. L. Magyar, K. McKeon, L. G. Goergen, C. Balliro, M. A. Hillard, D. M. Nathan, and E. R. Damiano, “Outpatient glycemic control with a bionic pancreas in type 1 diabetes,” *N Engl J Med*, vol. 371, pp. 313–325, 2014.
- [13] S. Del Favero, J. Place, J. Kropff, M. Messori, P. Keith-Hynes, R. Visentin, M. Munaro, D. Bruttomesso, S. Galasso, F. Boscari, C. Toffanin, F. Di Palma, G. Lanzola, S. Scarpellini, A. Ferret, B. Kovatchev, L. Magni, A. Avogaro, J. H. DeVries, C. Cobelli, and E. Renard on behalf of the AP@home Consortium, “Multicentre outpatient dinner/overnight reduction of hypoglycemia and increased time of glucose in target with a wearable artificial pancreas using multi-modular model predictive control algorithm in adults with type 1 diabetes,” *Diabetes Obes. Metab.*, vol. 17, no. 5, pp. 468–476, 2015.
- [14] H. Thabit, A. Lubina-Solomon, M. Stadler, L. Leelarathna, E. Walkinshaw, A. Pernet, J. M. Allen, A. Iqbal, P. Choudhary, K. Kumareswaran, M. Nodale, C. Nisbet, M. E. Wilinska, K. D. Barnard, D. B. Dunger, S. R. Heller, S. A. Amiel, M. L. Evans, and R. Hovorka, “Home use of closed-loop insulin delivery for overnight glucose control in adults with type 1 diabetes: a 4-week, multicentre, randomised crossover study,” *Lancet Diabetes Endocrinol.*

vol. 2, no. 9, pp. 701–709, 2014.

- 2 [15] J. Kropff, S. Del Favero, J. Place, C. Toffanin, R. Visentin, M. Monaro, M. Messori, F. Di  
Palma, G. Lanzola, A. Farret, F. Boscari, S. Galasso, P. Magni, A. Avogaro, P. Keith-Hynes,  
4 B. P. Kovatchev, D. Bruttomesso, C. Cobelli, J. H. DeVries, E. Renard, and L. Magni for  
the AP@home consortium, “2 month evening and night closed-loop glucose control in  
6 patients with type 1 diabetes under free-living conditions: a randomised crossover trial,”  
*Lancet Diabetes Endocrinol*, vol. 3, no. 12, pp. 939–947, 2015.
- 8 [16] L. Magni, D. M. Raimondo, L. Bossi, C. Dalla Man, G. De Nicolao, B. Kovatchev, and  
C. Cobelli, “Model predictive control of type 1 diabetes: an in silico trial,” *J Diabetes Sci  
10 Technol*, vol. 1, no. 6, pp. 804–812, 2007.
- [17] M. E. Wilinska, E. S. Budiman, M. B. Taub, D. Elleri, J. M. Allen, C. L. Acerini, D. B.  
12 Dunger, and R. Hovorka, “Overnight closed-loop insulin delivery with model predictive  
control: assessment of hypoglycemia and hyperglycemia risk using simulation studies,” *J  
14 Diabetes Sci Technol*, vol. 3, no. 5, pp. 1109–1120, 2009.
- [18] B. Grosman, E. Dassau, H. C. Zisser, L. Jovanovič, and F. J. Doyle III, “Zone model  
16 predictive control: a strategy to minimize hyper- and hypoglycemic events,” *J Diabetes Sci  
Technol*, vol. 4, no. 4, pp. 961–975, 2010.
- 18 [19] S. D. Patek, L. Magni, E. Dassau, C. Hughes-Karvetski, C. Toffanin, G. De Nicolao, S. Del  
Favero, M. Breton, C. Dalla Man, E. Renard, H. Zisser, F. J. Doyle, C. Cobelli, and B. P.  
20 Kovatchev, “Modular closed-loop control of diabetes,” *IEEE Trans. Biomed. Eng.*, vol. 59,  
no. 11, pp. 2986–2999, 2012.
- 22 [20] P. Soru, G. De Nicolao, C. Toffanin, C. Dalla Man, C. Cobelli, and L. Magni on behalf of  
the AP@home consortium, “Mpc based artificial pancreas: strategies for individualization  
24 and meal compensation,” *Annu Rev Control*, vol. 36, no. 1, pp. 118–128, 2012.
- [21] B. P. Kovatchev, C. Cobelli, E. Renard, S. Anderson, M. Breton, S. Patek, W. Clarke,  
26 D. Bruttomesso, A. Maran, S. Costa, A. Avogaro, C. Dalla Man, A. Facchinetti, L. Magni,  
G. De Nicolao, J. Place, and A. Farret, “Multinational study of subcutaneous model-  
28 predictive closed-loop control in type 1 diabetes mellitus: summary of the results,” *J  
Diabetes Sci Technol*, vol. 4, no. 6, pp. 1374–1381, 2010.
- 30 [22] R. Hovorka, K. Kumareswaran, J. Harris, J. M. Allen, D. Elleri, D. Xing, C. Kollman,  
M. Nodale, H. R. Murphy, D. B. Dunger, S. A. Amiel, S. R. Heller, M. E. Wilinska, and  
32 M. L. Evans, “Overnight closed loop insulin delivery (artificial pancreas) in adults with  
type 1 diabetes: crossover randomised controlled studies,” *BMJ*, 2011. [Online]. Available:  
34 <http://dx.doi.org/10.1136/bmj.d1855>
- [23] E. Dassau, H. Zisser, R. A. Harvey, M. W. Percival, B. Grosman, W. Bevier, E. Atlas,  
36 S. Miller, R. Nimri, L. Jovanovič, and F. J. Doyle III, “Clinical evaluation of a personalized  
artificial pancreas,” *Diabetes Care*, vol. 36, no. 4, pp. 801–809, 2013.

- [24] H. Zisser, E. Renard, B. Kovatchev, C. Cobelli, A. Avogaro, R. Nimri, L. Magni, B. Buckingham, H. P. Chase, F. J. Doyle III, J. Lum, P. Calhoun, C. Kollman, E. Dassau, A. Farret, J. Place, M. Breton, S. Anderson, C. Dalla Man, S. Del Favero, D. Bruttomesso, A. Filippi, R. Scotton, M. Phillip, E. Atlas, I. Muller, S. Miller, C. Toffanin, D. M. Raimondo, G. De Nicolao, and R. W. Beck for the control to range study group, “Multicenter closed-loop insulin delivery study points to challenges for keeping blood glucose in a safe range by a control algorithm in adults and adolescents with type 1 diabetes from various sites,” *Diabetes Technol Ther*, vol. 16, no. 10, pp. 613–622, 2014.
- [25] H. P. Chase, F. J. Doyle III, H. Zisser, E. Renard, R. Nimri, C. Cobelli, B. A. Buckingham, D. M. Maahs, S. Anderson, L. Magni, J. Lum, P. Calhoun, C. Kollman, and R. W. Beck for the Control to Range Study Group, “Multicenter closed-loop/hybrid meal bolus insulin delivery with type 1 diabetes,” *Diabetes Technol Ther*, vol. 16, no. 10, pp. 623–632, 2014.
- [26] Y. M. Luijf, J. H. DeVries, K. Zwinderman, L. Leelarathna, M. Nodale, K. Caldwell, K. Kumareswaran, D. Elleri, J. M. Allen, M. E. Wilinska, M. L. Evans, R. Hovorka, W. Doll, M. Ellmerer, J. K. Mader, E. Renard, J. Place, A. Farret, C. Cobelli, S. Del Favero, C. Dalla Man, A. Avogaro, D. Bruttomesso, A. Filippi, R. Scotton, L. Magni, G. Lanzola, F. Di Palma, P. Soru, C. Toffanin, G. De Nicolao, S. Arnolds, C. Benesch, and L. Heinemann, “Day and night closed-loop control in adults with type 1 diabetes mellitus: a comparison of two closed-loop algorithms driving continuous subcutaneous insulin infusion versus patient self-management,” *Diabetes Care*, vol. 36, no. 12, pp. 3882–3887, 2013.
- [27] C. Toffanin, M. Messori, F. Di Palma, G. De Nicolao, C. Cobelli, and L. Magni, “Artificial pancreas: model predictive control design from clinical experience,” *J Diabetes Sci Technol*, vol. 7, no. 6, pp. 1470–1483, 2013.
- [28] B. P. Kovatchev, E. Renard, C. Cobelli, H. C. Zisser, P. Keith-Hynes, S. M. Anderson, S. A. Brown, D. R. Chernavvsky, M. D. Breton, L. B. Mize, A. Farret, J. Place, D. Bruttomesso, S. Del Favero, F. Boscari, S. Galasso, A. Avogaro, L. Magni, F. Di Palma, C. Toffanin, M. Messori, E. Dassau, and F. J. Doyle III, “Safety of outpatient closed-loop control: first randomized crossover trials of a wearable artificial pancreas,” *Diabetes Care*, vol. 37, no. 7, pp. 1789–1796, 2014.
- [29] E. Renard, A. Farret, J. Kropff, D. Bruttomesso, M. Messori, J. Place, R. Visentin, R. Calore, C. Toffanin, F. Di Palma, G. Lanzola, P. Magni, F. Boscari, S. Galasso, A. Avogaro, P. Keith-Hynes, B. Kovatchev, S. Del Favero, C. Cobelli, L. Magni, and J. H. DeVries for the AP@home Consortium, “Day and night closed-loop glucose control in patients with type 1 diabetes under free-living conditions: results of a single-arm 1-month experience compared with a previously reported feasibility study of evening and night at home,” *Diabetes Care*, vol. 39, no. 7, pp. 1151–1160, 2016.
- [30] P. Palumbo, G. Pizzichelli, S. Panunzi, P. Pepe, and A. De Gaetano, “Model-based control

of plasma glycemia: Tests on populations of virtual patients,” *Math Biosci*, vol. 257, pp. 2–10, 2014.

- [31] R. Hovorka, V. Canonico, L. J. Chassin, U. Haueter, M. Massi-Benedetti, M. Orsini Federici, T. R. Pieber, H. C. Schaller, L. Schaupp, T. Vering, and M. E. Wilinska, “Nonlinear model predictive control of glucose concentration in subjects with type 1 diabetes,” *Physiol Meas*, vol. 25, no. 4, pp. 905–920, 2004.
- [32] C. Dalla Man, R. A. Rizza, and C. Cobelli, “Meal simulation model of the glucose-insulin system,” *IEEE Trans. Biomed. Eng.*, vol. 54, no. 10, pp. 1740–1749, 2007.
- [33] C. Dalla Man, D. M. Raimondo, R. A. Rizza, and C. Cobelli, “Gim, simulation software of meal glucose-insulin model,” *J Diabetes Sci Technol*, vol. 1, no. 3, pp. 323–330, 2007.
- [34] B. P. Kovatchev, M. D. Breton, C. Dalla Man, and C. Cobelli, “In silico preclinical trials: a proof of concept in closed-loop control of type 1 diabetes,” *J Diabetes Sci Technol*, vol. 3, no. 1, pp. 44–55, 2009.
- [35] C. Dalla Man, F. Micheletto, D. Lv, M. Breton, B. Kovatchev, and C. Cobelli, “The UVA/Padova type 1 diabetes simulator: New features,” *J Diabetes Sci Technol*, vol. 8, no. 1, pp. 26–34, 2014.
- [36] R. Visentin, C. Dalla Man, B. Kovatchev, and C. Cobelli, “The university of virginia/padova type 1 diabetes simulator matches the glucose traces of a clinical trial,” *Diabetes Technol Ther*, vol. 16, no. 7, pp. 428–434, 2014.
- [37] R. Visentin, C. Dalla Man, Y. C. Kudva, A. Basu, and C. Cobelli, “Circadian variability of insulin sensitivity: physiological input for in silico artificial pancreas,” *Diabetes Technol Ther*, vol. 17, no. 1, pp. 1–7, 2015.
- [38] R. Visentin, C. Dalla Man, and C. Cobelli, “One-day bayesian cloning of type 1 diabetes subjects: towards a single-day UVA/Padova type 1 diabetes simulator,” *IEEE Trans Biomed Eng*, vol. 63, no. 11, pp. 2416–2424, 2016.
- [39] S. Del Favero, F. Boscari, M. Messori, I. Rabbone, R. Bonfanti, A. Sabbion, D. Iafusco, R. Schiaffini, R. Visentin, R. Calore, Y. Leal Moncada, S. Galasso, A. Galderisi, V. Vallone, F. Di Palma, E. Losiouk, G. Lanzola, D. Tinti, A. Rigamonti, M. Marigliano, A. Zanfardino, N. Rapini, A. Avogaro, D. Chernavvsky, L. Magni, C. Cobelli, and D. Bruttomesso, “Randomized summer camp cross-over trial in 5–9 year old children: outpatient wearable artificial pancreas is feasible and safe,” *Diabetes Care*, vol. 39, no. 7, pp. 1180–1185, 2016.
- [40] M. Messori, M. Ellis, C. Cobelli, P. D. Christofides, and L. Magni, “Improved postprandial glucose control with a customized model predictive controller,” in *American Control Conference (ACC)*, Chicago, IL, USA, July 1–3 2015, pp. 5108–5115.
- [41] M. Messori, C. Toffanin, S. Del Favero, G. De Nicolao, C. Cobelli, and L. Magni, “Model individualization for artificial pancreas,” *Comput Meth Prog Bio*, 2016. [Online]. Available: <http://dx.doi.org/10.1016/j.cmpb.2016.06.006>

- [42] G. Pillonetto and G. De Nicolao, “A new kernel-based approach for linear system identification,” *Automatica*, vol. 46, no. 1, pp. 81–93, 2010.
- [43] S. Del Favero, A. Facchinetti, G. Sparacino, and C. Cobelli, “Improving accuracy and precision of glucose sensor profiles: retrospective fitting by constrained deconvolution,” *IEEE Trans. Biomed. Eng.*, vol. 61, no. 4, pp. 1044–1053, 2014.
- [44] M. Messori, C. Toffanin, S. Del Favero, G. De Nicolao, C. Cobelli, and L. Magni, “A nonparametric approach for model individualization in an artificial pancreas,” *IFAC-PapersOnLine*, vol. 48, no. 20, pp. 225–230, 2015.
- [45] C. Ellingsen, E. Dassau, H. Zisser, B. Grosman, M. W. Percival, L. Jovanovič, and F. J. Doyle III, “Safety constraints in an artificial pancreatic beta cell: an implementation of model predictive control with insulin on board,” *J Diabetes Sci Technol*, vol. 3, no. 3, pp. 536–544, 2009.
- [46] L. Magni, D. M. Raimondo, C. Dalla Man, M. Breton, S. Patek, G. De Nicolao, C. Cobelli, and B. P. Kovatchev, “Evaluating the efficacy of closed-loop glucose regulation via control-variability grid analysis,” *J Diabetes Sci Technol*, vol. 2, no. 4, pp. 630–635, 2008.
- [47] D. M. Maahs, B. A. Buckingham, J. R. Castle, A. Cinar, E. R. Damiano, E. Dassau, J. H. DeVries, F. J. Doyle III, S. C. Griffen, A. Haidar, L. Heinemann, R. Hovorka, T. W. Jones, C. Kollman, B. Kovatchev, B. L. Levy, R. Nimri, D. N. O’Neal, M. Philip, E. Renard, S. J. Russell, S. A. Weinzimer, H. Zisser, and J. W. Lum, “Outcome measures for artificial pancreas clinical trials: a consensus report,” *Diabetes Care*, vol. 39, no. 7, pp. 1175–1179, 2016.

TABLE 1. State variables associated with the state space system (1)

State	Meaning	Unit
$x_1$	Stomach first compartment	mg
$x_2$	Stomach second compartment	mg
$x_3$	Intestine	mg
$x_4$	Plasma glucose & insulin-independent tissues	mg/kg
$x_5$	Insulin-dependent tissues	mg/kg
$x_6$	Plasma insulin	pmol/kg
$x_7$	Insulin action	pmol/l
$x_8$	Delay compartment for insulin action on glucose production	pmol/l
$x_9$	Insulin action on glucose production	pmol/l
$x_{10}$	Insulin in the liver	pmol/kg
$x_{11}$	First compartment of subcutaneous insulin	pmol/kg
$x_{12}$	Second compartment of subcutaneous insulin	pmol/kg
$x_{13}$	Subcutaneous glucose	mg/kg
$x_{14}$	Plasma glucagon	ng/dl
$x_{15}$	Glucagon action	ng/dl
$x_{16}$	Delayed static glucagon secretion	ng/dl/min

TABLE 2. Inputs, output, and key metabolic parameters associated with the state space system (1)

	Symbol	Meaning	Unit
Model inputs	$i(t)$	Exogenous insulin infusion rate	pmol/kg/min
	$d(t)$	Ingested meal	mg/min
Model output	$\frac{x_{13}(t)}{V_G}$	Subcutaneous glucose concentration	mg/dl
Constant parameters	$k_{gri}, k_{abs}$ $k_1, k_2, k_{a1}, k_{a2}$ $m_1, m_2, m_4, p_{2U}$ $k_i, k_d, k_{sc}, k_H, n_G$	Rate parameters	$\text{min}^{-1}$
	$V_I$	Distribution volume of insulin	l/kg
	$V_G$	Distribution volume of glucose	dl/kg
	$I_b$	Model basal insulin	pmol/l
	$H_b$	Model basal glucagon	ng/dl
Time-varying parameters	$k_{empt}(t)$	Gastric emptying coefficient	$\text{min}^{-1}$
	$Ra(t)$	Glucose rate of appearance	mg/kg/min
	$EGP(t)$	Endogenous glucose production	mg/kg/min
	$E(t)$	Renal excretion	mg/kg/min
	$U_{ii}(t)$	Insulin independent utilization	mg/kg/min
	$U_{id}(t)$	Insulin dependent utilization	mg/kg/min
	$m_3(t)$	Linear degradation coefficient	$\text{min}^{-1}$
	$SR_H(t)$	Glucagon secretion	ng/dl/min
	$SR_H^s(t)$	Delayed static glucagon secretion	ng/dl



TABLE 3. Closed-loop performance indices achieved by L-MPC, CR-MPC, NP-MPC, and CO-MPC in the simulation scenario of Figure 8. O is the overall scenario, N is night, and PP are closed-loop postprandial periods.

		O	N	PP
A (mg/dl)	L-MPC	144.85 (126.81, 158.88)	121.75 (113.90, 127.70)	155.83 (29.85)
	CR-MPC	144.10 (126.47, 155.66) <sup>††</sup>	122.07 (113.98, 127.78) <sup>††</sup>	154.13 (26.76) <sup>††</sup>
	NP-MPC	133.34 (118.73, 145.23) <sup>†††</sup>	114.57 (108.30, 119.36) <sup>†††</sup>	144.88 (26.17) <sup>†††</sup>
	CO-MPC	136.95 (123.97, 148.12) <sup>†††</sup>	116.03 (110.73, 122.56) <sup>†††</sup>	152.24 (26.01) <sup>†</sup>
SD (mg/dl)	L-MPC	21.41 (17.18, 27.45)	6.68 (4.35, 10.47)	19.95 (15.95, 25.13)
	CR-MPC	21.50 (16.63, 26.77) <sup>†††</sup>	6.25 (3.99, 9.04) <sup>†††</sup>	19.72 (15.79, 24.69)
	NP-MPC	22.11 (17.96, 27.46)	5.04 (3.09, 7.24) <sup>†††</sup>	21.41 (18.52, 25.91) <sup>†††</sup>
	CO-MPC	22.66 (18.85, 29.01) <sup>††</sup>	5.50 (3.74, 8.06) <sup>††</sup>	22.35 (18.54, 26.93) <sup>†††</sup>
CV (mg/dl)	L-MPC	0.16 (0.13, 0.19)	0.06 (0.04, 0.08)	0.13 (0.05)
	CR-MPC	0.16 (0.13, 0.18) <sup>††</sup>	0.05 (0.03, 0.08) <sup>†</sup>	0.13 (0.05)
	NP-MPC	0.17 (0.14, 0.21) <sup>†††</sup>	0.04 (0.03, 0.06) <sup>††</sup>	0.16 (0.05) <sup>†††</sup>
	CO-MPC	0.17 (0.14, 0.20) <sup>†††</sup>	0.05 (0.03, 0.07) <sup>†</sup>	0.16 (0.05) <sup>†††</sup>
Tt (%)	L-MPC	95.18 (75.66, 100.00)	100.00 (100.00, 100.00)	90.57 (57.86, 100.00)
	CR-MPC	95.65 (81.23, 100.00) <sup>†</sup>	100.00 (100.00, 100.00)	91.72 (66.61, 100.00) <sup>†</sup>
	NP-MPC	97.37 (87.95, 100.00) <sup>†††</sup>	100.00 (100.00, 100.00)	95.16 (78.96, 100.00) <sup>†††</sup>
	CO-MPC	95.24 (82.25, 100.00)	100.00 (100.00, 100.00)	90.47 (69.11, 100.00)
Ttt (%)	L-MPC	46.17 (24.98)	100.00 (87.89, 100.00)	16.93 (6.61, 66.82)
	CR-MPC	48.70 (24.41) <sup>†</sup>	100.00 (91.23, 100.00) <sup>†</sup>	26.51 (8.39, 66.77) <sup>†</sup>
	NP-MPC	65.17 (21.07) <sup>†††</sup>	100.00 (100.00, 100.00) <sup>†††</sup>	45.83 (22.81, 70.42) <sup>†††</sup>
	CO-MPC	59.36 (23.68) <sup>†††</sup>	100.00 (100.00, 100.00) <sup>†</sup>	35.26 (15.36, 62.34) <sup>††</sup>
Ta (%)	L-MPC	4.35 (0.00, 24.34)	0.00 (0.00, 0.00)	8.02 (0.00, 42.14)
	CR-MPC	3.67 (0.00, 18.77) <sup>†</sup>	0.00 (0.00, 0.00)	6.41 (0.00, 33.13) <sup>†</sup>
	NP-MPC	1.67 (0.00, 12.05) <sup>†††</sup>	0.00 (0.00, 0.00)	3.33 (0.00, 20.05) <sup>†††</sup>
	CO-MPC	4.35 (0.00, 17.75)	0.00 (0.00, 0.00)	8.70 (0.00, 30.89)
Tb (%)	L-MPC	0.00 (0.00, 0.00)	0.00 (0.00, 0.00)	0.00 (0.00, 0.00)
	CR-MPC	0.00 (0.00, 0.00)	0.00 (0.00, 0.00)	0.00 (0.00, 0.00)
	NP-MPC	0.00 (0.00, 0.00)	0.00 (0.00, 0.00)	0.00 (0.00, 0.00)
	CO-MPC	0.00 (0.00, 0.00)	0.00 (0.00, 0.00)	0.00 (0.00, 0.00)
#ht	L-MPC	9	0	9
	CR-MPC	18	0	18
	NP-MPC	18	0	15
	CO-MPC	2	0	2
# patients with ht	L-MPC	4	0	4
	CR-MPC	4	0	4
	NP-MPC	5	0	5
	CO-MPC	1	0	1
Daily insulin needs (U)	L-MPC	47.35 (39.15, 59.08)	9.35 (8.06, 10.92)	46.29 (35.39, 53.52)
	CR-MPC	49.75 (39.50, 62.90) <sup>†††</sup>	9.68 (7.99, 10.91)	48.49 (36.28, 59.36) <sup>††</sup>
	NP-MPC	51.18 (41.10, 63.55) <sup>††</sup>	10.09 (8.46, 12.10) <sup>†††</sup>	44.39 (36.01, 56.77)
	CO-MPC	42.70 (36.63, 51.70) <sup>†††</sup>	9.35 (8.01, 11.24)	36.52 (31.07, 45.74) <sup>†††</sup>
Daily insulin needs per kg (U/kg)	L-MPC	0.69 (0.59, 0.86)	0.14 (0.12, 0.17)	0.65 (0.53, 0.83)
	CR-MPC	0.76 (0.60, 0.92) <sup>†††</sup>	0.14 (0.12, 0.17)	0.70 (0.54, 0.85) <sup>†††</sup>
	NP-MPC	0.76 (0.61, 0.95) <sup>††</sup>	0.14 (0.12, 0.18) <sup>†††</sup>	0.67 (0.52, 0.86)
	CO-MPC	0.62 (0.52, 0.76) <sup>†††</sup>	0.14 (0.11, 0.17)	0.53 (0.44, 0.69) <sup>†††</sup>

TABLE 4. Mean and standard deviation of the time below target achieved in closed-loop by L-MPC, CR-MPC, NP-MPC, and CO-MPC in the simulation scenario of Figure 8. O is the overall scenario, N is night, and PP are closed-loop postprandial periods.

		O	N	PP
Tb (%)	L-MPC	0.17 (0.80)	0.00 (0.00)	0.33 (1.61)
	CR-MPC	0.27 (1.51)	0.00 (0.00)	0.53 (3.02)
	NP-MPC	0.30 (1.35)	0.00 (0.00)	0.41 (2.29)
	CO-MPC	0.08 (0.56)	0.00 (0.00)	0.13 (1.06)

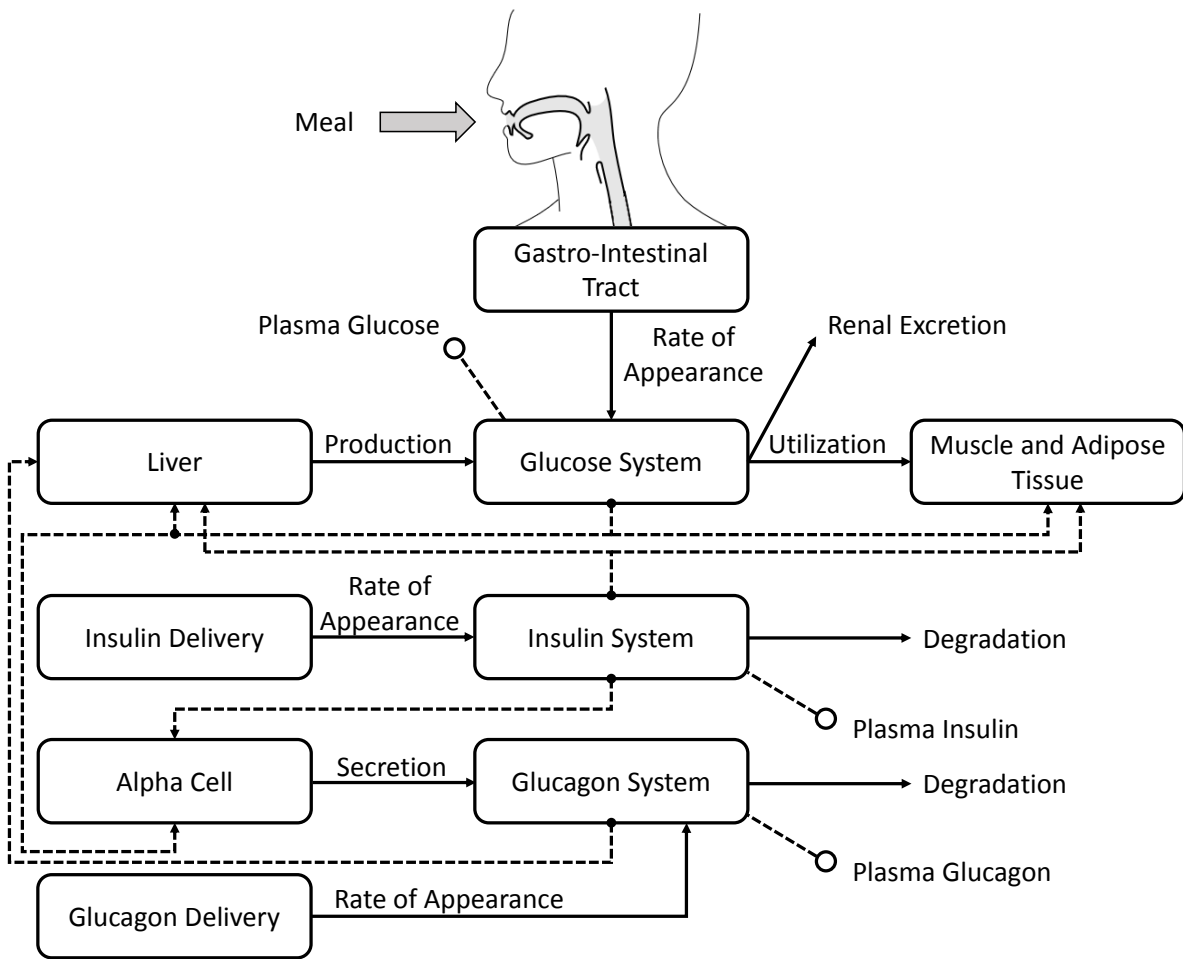


Figure 1. Compartmental representation of the glucose-insulin model included in the UVA/Padova simulator [35]. The fluxes of material are represented by the solid arrows, dashed arrows represent control signals between compartments, while dashed lines linked to empty circles represent the accessible compartments.

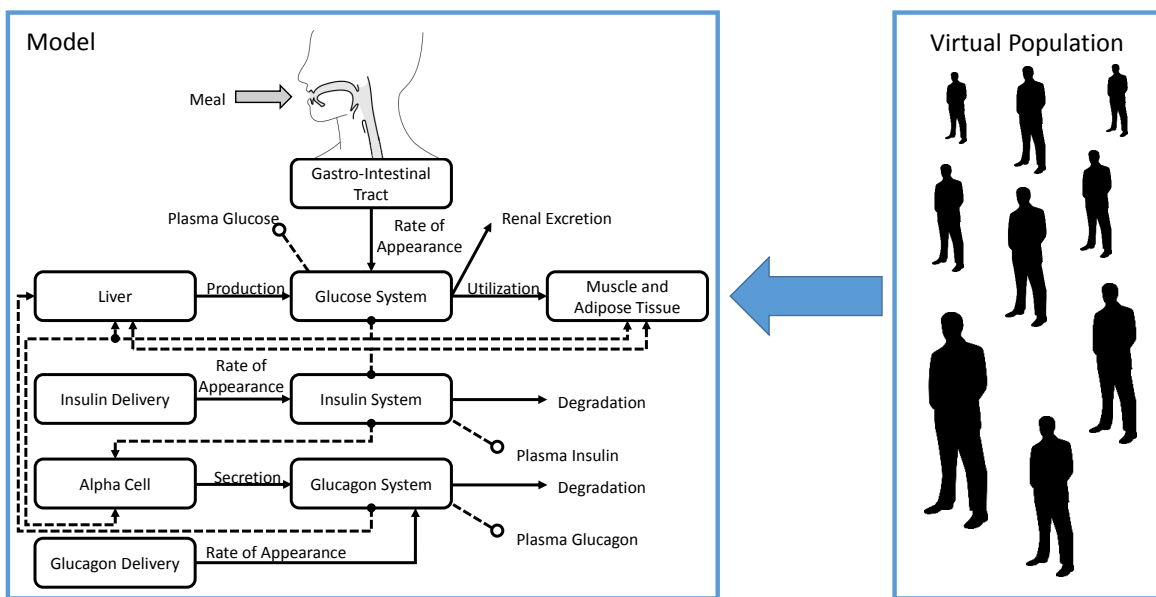


Figure 2. A virtual population is composed of several “virtual subjects”. Each virtual subject is characterized by a set of key metabolic parameters of the glucose-insulin model. A virtual population is thought to span the inter-subject variability that can be encountered in a population of patients affected by type 1 diabetes.

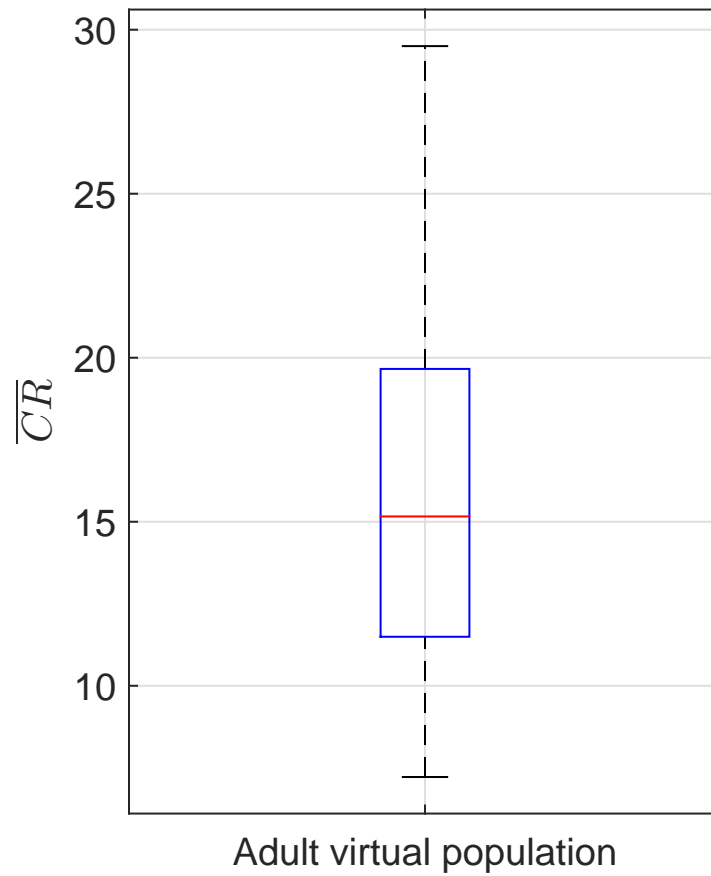


Figure 3. Distribution of the average daily Insulin-To-Carbo Ratio patterns ( $\overline{CR}$ ) associated with the adult virtual population of the UVA/Padova simulator. For each virtual subject, a pattern is known and used to build the boxplot, which is composed of 100 values. As specified in (4), the integer approximations of the 25-th, 50-th, and 75-th percentiles are equal to 12, 15, and 19, respectively.

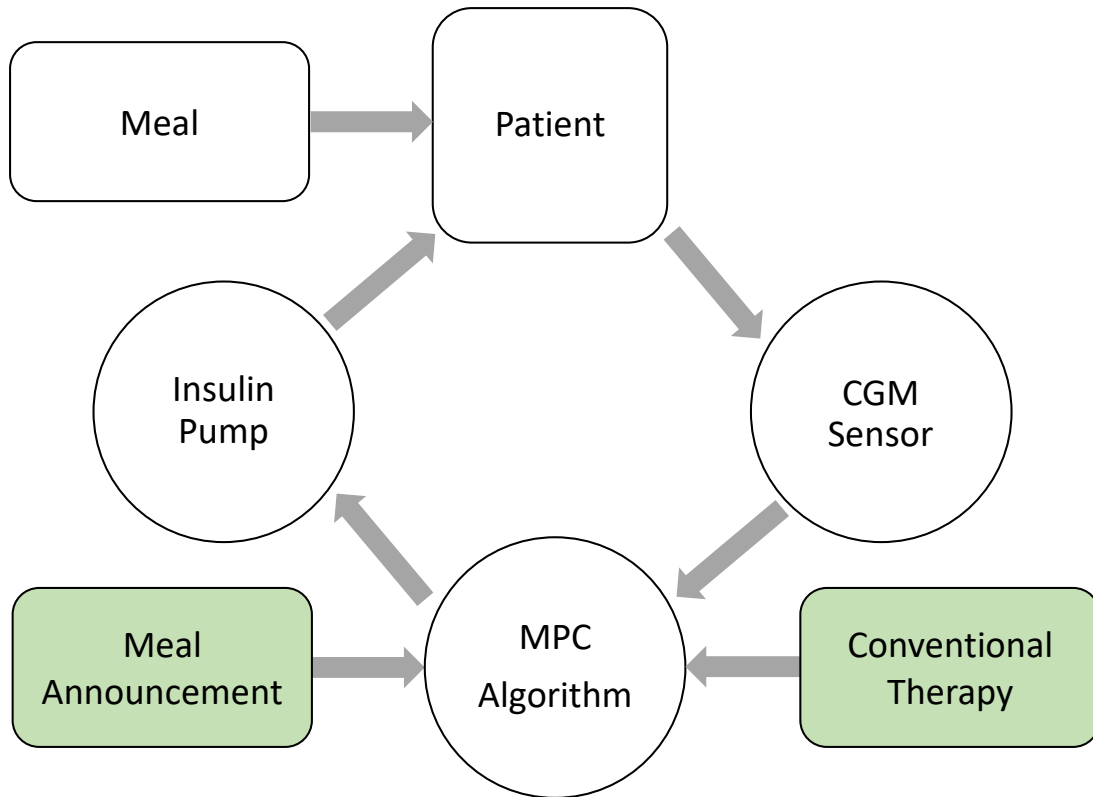


Figure 4. Schematic representation of an artificial pancreas. Circled elements represent the main components of the system, which are the continuous glucose monitor (CGM) sensor, the model predictive control (MPC) algorithm, and the subcutaneous insulin pump. The MPC algorithm relies on the patient conventional therapy and on the feedforward action associated with the meal announcement.

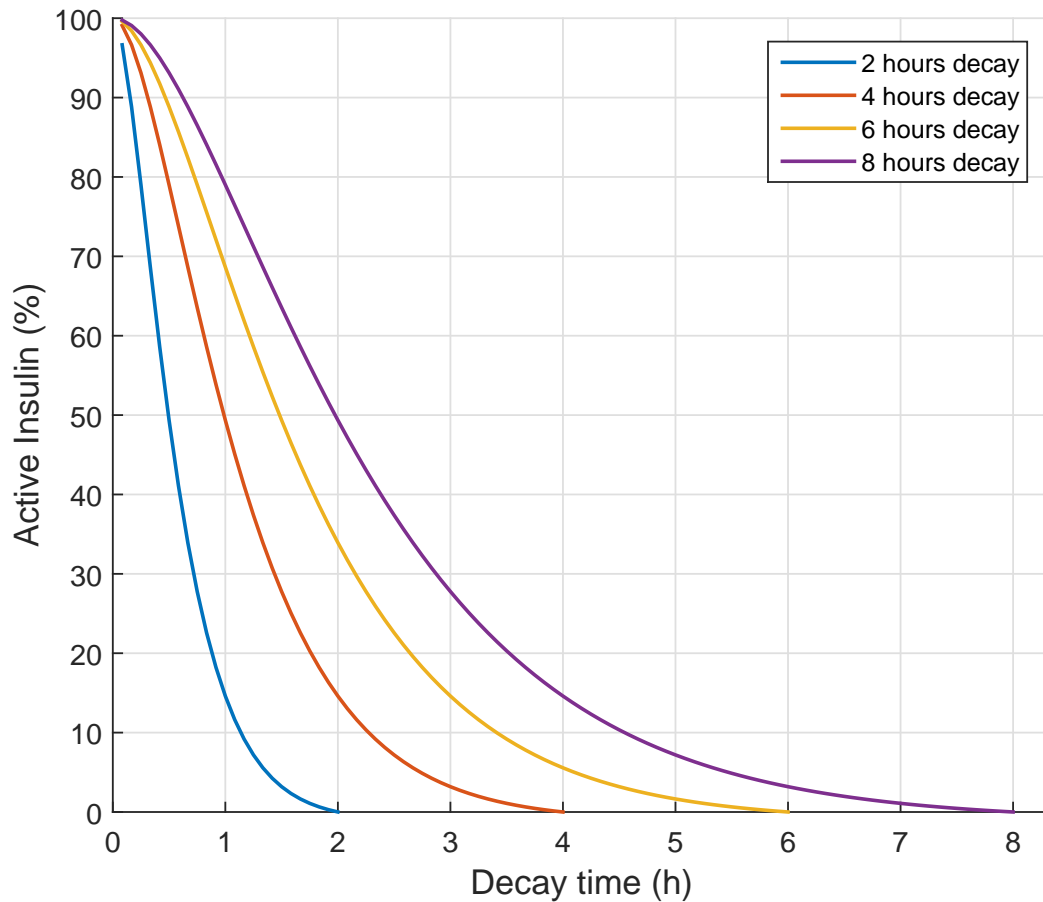


Figure 5. Insulin decay curves. Each curve is characterized by a time of decay of  $h$  hours, which determines the percentage of still active insulin in function of time. The active insulin is the insulin that has still to have an effect in the patient and is estimated through (10).

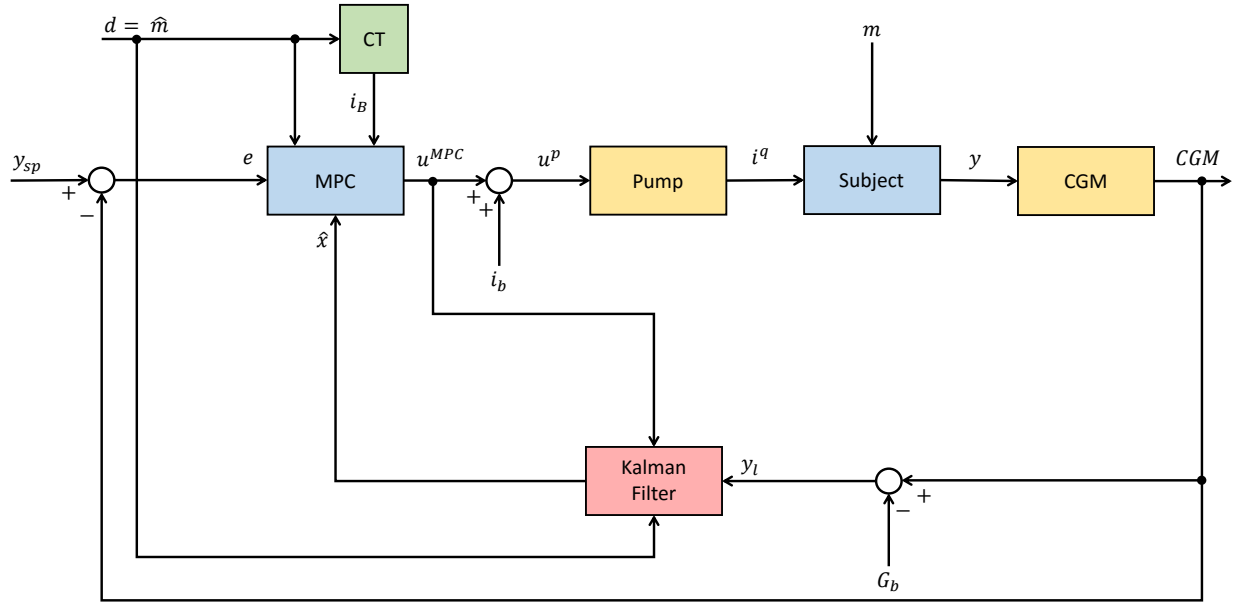


Figure 6. Closed-loop scheme implemented in the artificial pancreas system.  $d = \hat{m}$  is the estimated quantity of carbohydrates associated with the meal  $m$ , and it is considered in the feedforward action as a disturbance to be rejected. When a meal is announced, model predictive control (MPC) receives the estimation of the nominal insulin bolus  $i_B$  through (9), which is included in the conventional therapy (CT).  $y_{sp}$  is the glucose set-point,  $y$  is the noisy subcutaneous glucose measured by the continuous glucose monitor (CGM) device, and  $e = y_{sp} - CGM$  is the glucose error sent to the MPC.  $u^{MPC}$  is the suggested insulin variation with respect to the basal insulin  $i_b$ , and  $u^p$  is the insulin that has to be infused by the pump, which infuses the quantized insulin  $i^q$  into the patient subcutaneous tissue. MPC is fed also with the estimate patient state  $\hat{x}$ , which is estimated through the Kalman filter described in [27]. The latter uses the system inputs and the noisy output  $y_l = CGM - G_b$ , with  $G_b$  denoting the steady state glucose concentration during fasting periods (basal glucose).



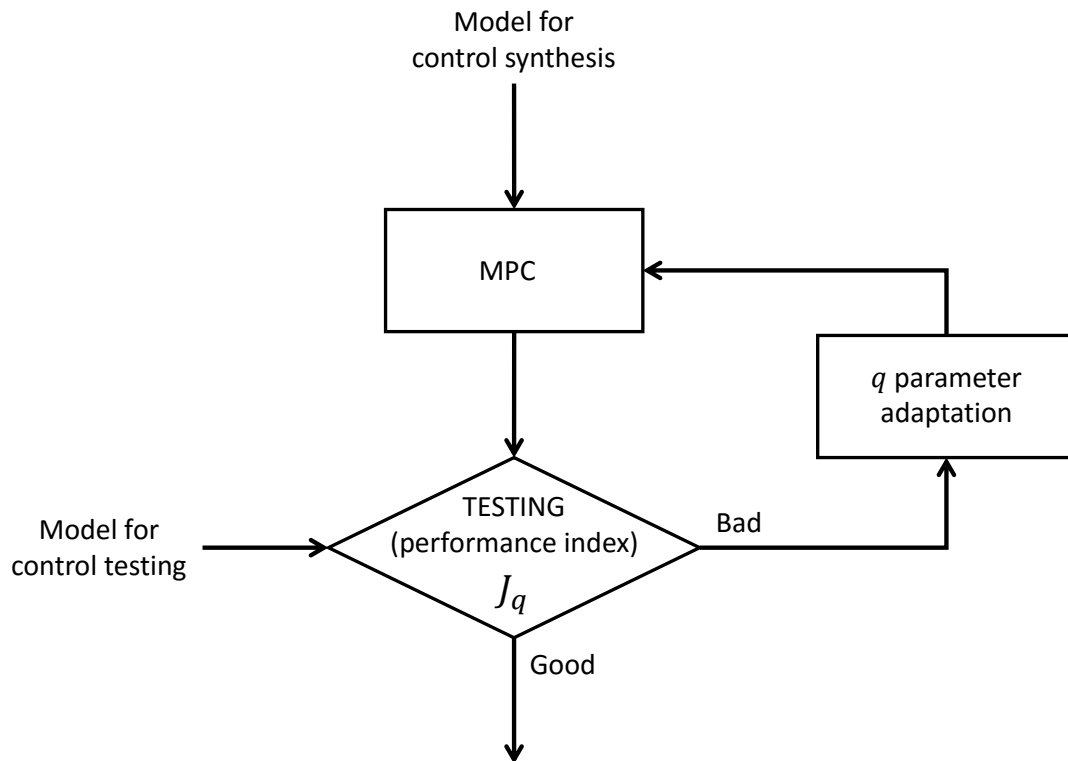


Figure 7. Flow chart of the calibration procedure used to tune the parameter  $q$  in the cost function (11). The model predictive control (MPC) is synthesized with the model for control synthesis and is used in a trial and error approach to simulate the closed-loop glucose control on the model for control testing. The process is iterated until the decrease on the performance index  $J_q$  defined in (12) becomes negligible.

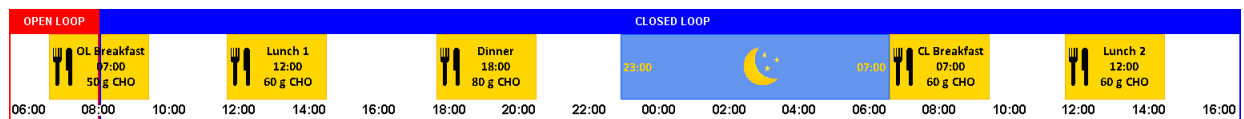


Figure 8. Scenario used for closed-loop (CL) simulations. The scenario starts at 6:00 and lasts 34 hours, and the loop is closed at 8:00. The first breakfast is compensated in open-loop (OL) through the conventional therapy, while the remaining meals are compensated in CL. The night starts at 23:00 and lasts eight hours. Meal amounts are 50 g of carbohydrates (CHO) for the first breakfast, 80 g CHO for the dinner, and 60 g CHO for the remaining meals.

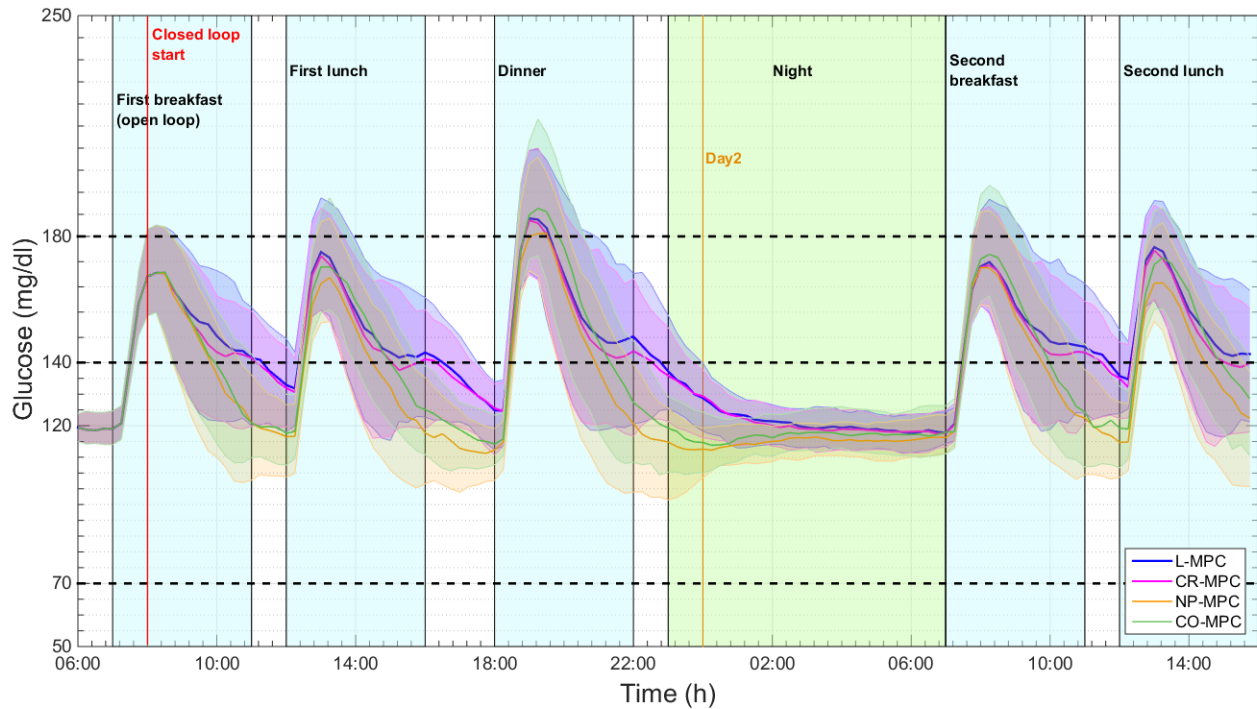


Figure 9. Blood glucose concentration achieved by the linearized non-individualized model predictive control (L-MPC), by the customized model predictive control synthesized with the Insulin-To-Carbo Ratio based models (CR-MPC), and by the individualized model predictive control synthesized by considering the nonparametric (NP-MPC), and the constrained optimization (CO-MPC) models in the simulation scenario of Figure 8. Glucose values are shown in terms of median (solid lines) surrounded by colored regions representing the glucose 25-th and 75-th percentiles.

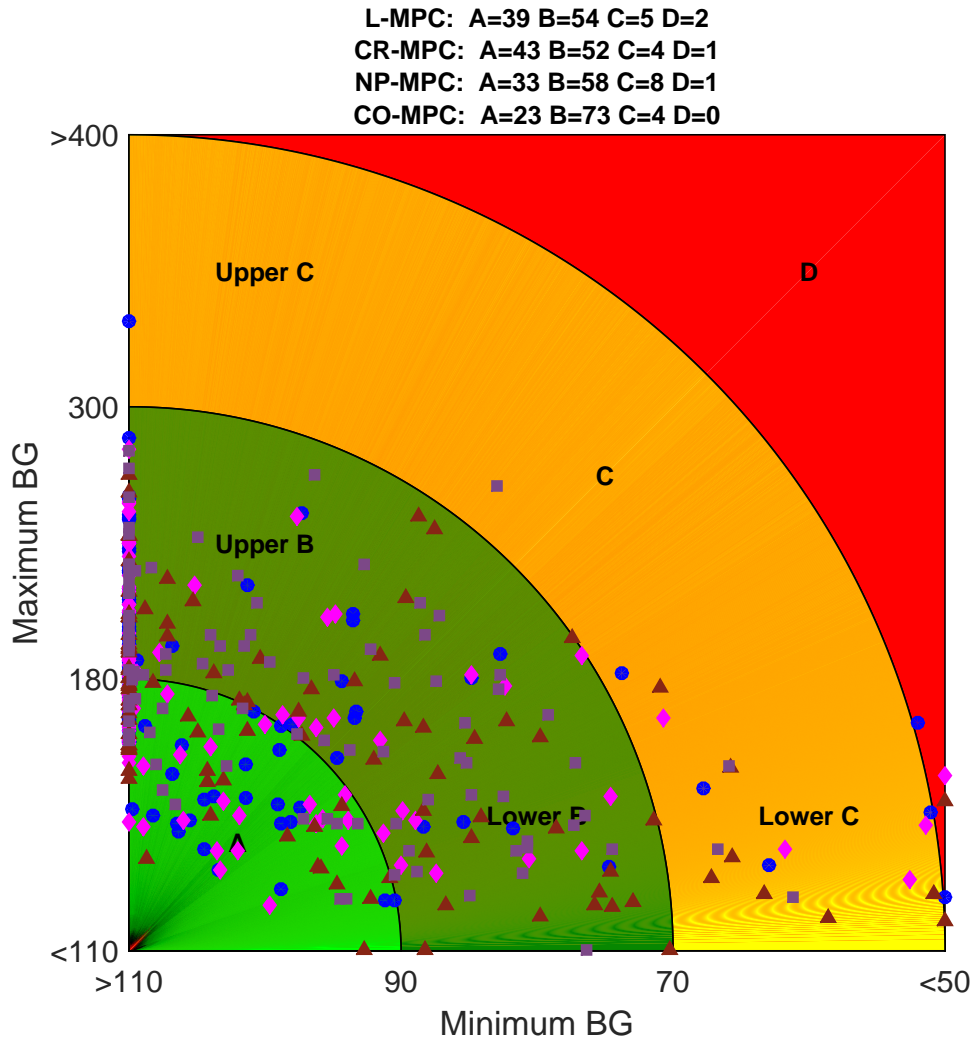


Figure 10. Control variability grid analysis [20] achieved by the linearized non-individualized model predictive control (L-MPC, blue circles), by the customized model predictive control synthesized with the Insulin-To-Carbo Ratio based models (CR-MPC, magenta diamonds), and by the individualized model predictive control synthesized by considering the nonparametric (NP-MPC, brown triangles), and the constrained optimization (CO-MPC, violet squares) models in the simulation scenario of Figure 8. Each point represents the combination of the minimum and maximum blood glucose (BG) reached by a virtual subject in simulation.

## Sidebar 1: Preliminaries on Model Predictive Control

In several application contexts, there is the need to perform particularly critical tasks while fulfilling some plant constraints. MPC is one of the most effective solutions to this problem, as it can comply with large scale systems with many control variables and provides a systematic method of dealing with constraints on inputs and states. MPC constraints are explicitly taken into account by solving an online constrained optimization problem used to determine the optimal inputs with respect to a predefined cost function. Typically, the optimization problem and the control law are defined in discrete-time domain, and the major ingredients needed for its implementation are the model of the plant and a cost function to optimize.

Consider the discrete-time linear system

$$x(k+1) = Ax(k) + Bu(k) + Md(k), \quad (\text{S1})$$

where  $x(k) \in \mathbb{R}^n$  is the state vector,  $u(k) \in \mathbb{R}^m$  is the input vector, and  $d(k) \in \mathbb{R}^l$  is a disturbance vector at the  $k$ -th sampling time instant,  $A \in \mathbb{R}^{n \times n}$ ,  $B \in \mathbb{R}^{n \times m}$ , and  $M \in \mathbb{R}^{n \times l}$ . Let  $N$  denote the prediction horizon. Given a predicted input sequence

$$U(k) = [u^T(k|k), u^T(k+1|k), \dots, u^T(k+N-1|k)]^T,$$

and a disturbance sequence

$$D(k) = [d^T(k), d^T(k+1), \dots, d^T(k+N-1)]^T,$$

the time evolution of the state is generated by simulating the model (S1) forward for  $N$  sampling time intervals with initial condition  $x(k|k) = x(k)$ . Consequently,

$$X(k+1) = [x^T(k+1|k), x^T(k+2|k), \dots, x^T(k+N|k)]^T,$$

with  $u(k+i|k)$  and  $x(k+i|k)$ ,  $i \in \mathbb{N}$ , being the input and state at time  $k+i$  predicted at time  $k$ .

The control input fed into the plant is generated by solving an optimization problem driven by a pre-specified cost function to be minimized, for instance:

$$J(x(k), U(\cdot), k) = \sum_{i=0}^{N-1} \|x(k+i|k) - x_{ref}(k+i)\|_Q^2 + \|u(k+i|k) - u_{ref}(k+i)\|_R^2, \quad (\text{S2})$$

with  $x_{ref}(k)$  and  $u_{ref}(k)$  denoting the states and inputs references at time  $k$ , respectively, included in the reference vectors

$$\begin{aligned} U_{ref}(k) &= [u_{ref}^T(k), u_{ref}^T(k+1), \dots, u_{ref}^T(k+N-1)]^T, \\ X_{ref}(k) &= [x_{ref}^T(k), x_{ref}^T(k+1), \dots, x_{ref}^T(k+N-1)]^T, \end{aligned} \quad (\text{S3})$$

and where  $Q$  and  $R$  are symmetric positive definite matrices. The goal is to find the optimal control sequence  $U^o(k)$  such that

$$U^o(k) = \arg \min_U J(x(k), U(\cdot), k) ,$$

subject to the model (S1) and possibly including input and state constraints.

Finally, after the generation of the control input and according to the receding horizon approach, only the first element of the optimal control sequence  $U^o(k)$  is fed into the plant:

$$u(k) = u^o(k|k) .$$

2 The optimization process is then repeated at each sampling time  $k$ .

As previously discussed, one of the features of MPC is the presence of input and state  
4 constraints in the optimization problem. In addition to the equality constraints representing the  
model dynamics (S1), inequality constraints on input and state variables can be introduced. While  
6 the equality constraints are usually handled implicitly to compute predicted state trajectories as  
functions of initial conditions and input trajectories, the inequality constraints are explicitly  
8 imposed within the optimization problem.

The cost function defined in (S2) can be enriched with a weight associated with the state  
10 prediction at the horizon  $N$ . This modification can be performed by considering the quadratic  
cost function

$$J(x(k), U(\cdot), k) = \sum_{i=0}^{N-1} \|x(k+i|k) - x_{ref}(k+i)\|_Q^2 + \|u(k+i|k) - u_{ref}(k+i)\|_R^2 \quad (\text{S4})$$

$$+ \|x(k+N|k)\|_P^2 ,$$

12 subject to the state dynamics (S1), with  $P$  being the unique nonnegative solution of the discrete  
time Riccati equation

$$P(k) = Q + A^T P(k+1)A - A^T P(k+1)B (R + B^T P(k+1)B)^{-1} B^T P(k+1)A . \quad (\text{S5})$$

The matrix  $P \in \mathbb{R}^{n \times n}$  is the weight related to the term  $x(k+N|k)$ , which represents the predicted  
state at the horizon  $N$ .  $P$  takes into account the cost over an infinite horizon. By considering  
the horizon  $N$ , the predicted state trajectories of the system dynamics can be written as

$$X(k+1) = \mathcal{A}x(k) + \mathcal{B}U(k) + \mathcal{M}D(k) ,$$

where the matrices  $\mathcal{A} \in \mathbb{R}^{nN \times n}$ ,  $\mathcal{B} \in \mathbb{R}^{nN \times mN}$ , and  $\mathcal{M} \in \mathbb{R}^{nN \times lN}$  are obtained through algebraic  
calculations based on (S1). Of note, in the general case  $D(k)$  can be known, estimated, or  
unknown depending on the specific application to control. In case of unknown disturbance,  
the MPC calibration achieved through  $Q$  and  $R$  parameters of (S4) must be robust enough to

guarantee at least sub-optimal (but safe) control performance. Thus, the cost (S4) can be rewritten as

$$J(x(k), U(\cdot), k) = \|U(k)\|_{\mathcal{H}}^2 + 2 \left( x^T(k) \mathcal{F}_x^T + D^T(k) \mathcal{F}_D^T - U_{ref}^T(k) \mathcal{R} - X_{ref}^T(k) \mathcal{F}_{X_{ref}}^T \right) U(k) ,$$

where only the terms depending on  $U(k)$  have been maintained and where  $\mathcal{H} = \mathcal{B}^T \mathcal{Q} \mathcal{B} + \mathcal{R}$ ,  
 $\mathcal{F}_x = \mathcal{B}^T \mathcal{Q} \mathcal{A}$ ,  $\mathcal{F}_D = \mathcal{B}^T \mathcal{Q} \mathcal{M}$ , and  $\mathcal{F}_{X_{ref}} = \mathcal{B}^T \mathcal{Q}$ , with  $\mathcal{Q} = \text{diag}(Q, \dots, Q) \in \mathbb{R}^{nN \times nN}$  and  $\mathcal{R} = \text{diag}(R, \dots, R) \in \mathbb{R}^{mN \times mN}$ .

If the optimization problem does not take into account input and state constraints, under the assumption of non-singularity of the matrix  $\mathcal{H}$ , the solution exists, is unique, and can be explicitly written as

$$U^o(k) = \mathcal{H}^{-1} \left( -\mathcal{F}_x x(k) - \mathcal{F}_D D(k) + \mathcal{R} U_{ref}(k) + \mathcal{F}_{X_{ref}} X_{ref}(k) \right) .$$

4 On the other hand, in case of constraints on input or states, the optimization problem must be solved online through a quadratic programming optimizer.

## Sidebar 2: Compartmental Models

2 Compartmental models are represented by a set of compartments that can send control  
 signals to other compartments, and have the capability to contain some material that can be  
 4 exchanged with other compartments. The generic equation that describes the quantity of material  
 contained in a specific compartment is

$$\dot{Q}_m^i(t) = \sum_{\substack{j=1 \\ j \neq i}}^{N_c} R_{ij} - \sum_{\substack{j=1 \\ j \neq i}}^{N_c} R_{ji} , \quad i = 1, \dots, N_c , \quad (\text{S6})$$

6 where  $Q_m^i$  is the quantity of material of the  $i$ -th compartment,  $N_c$  is the total number of  
 compartments,  $R_{ij}$  is the incoming flux of material from compartment  $j$  to compartment  $i$ , and  
 8  $R_{ji}$  is the outgoing flux from compartment  $i$  to compartment  $j$ . A set of equations of the form of  
 (S6) describes the relationships among compartments, defining the whole system dynamics. The  
 10 flow rate between two compartments can be described by linear or nonlinear laws. Examples of  
 nonlinear laws are [S1]

$$\begin{aligned} R_{ij}(Q_m^j(t)) &= \frac{V_{max} \cdot Q_m^j(t)^{k_1-1}}{K_m + Q_m^j(t)^{k_1}} , \\ R_{ij}(Q_m^j(t)) &= \frac{V_{max}}{K_m + Q_m^j(t)} , \\ R_{ij}(Q_m^j(t)) &= \begin{cases} k_2(1 - \frac{Q_m^i(t)}{k_3}) & Q_m^i(t) < k_3 , \\ 0 & Q_m^i(t) \geq k_3 , \end{cases} \end{aligned} \quad (\text{S7})$$

12 where  $k_1$ ,  $k_2$  and  $k_3$  are constants, and  $K_m$  and  $V_{max}$  are rate parameters. The flux can be also  
 described by a linear relationship

$$R_{ij}(Q_m^j(t)) = k_{ij}Q_m^j(t) , \quad (\text{S8})$$

14 where  $k_{ij}$  is the rate constant associated with the incoming flux from compartment  $j$  to  
 compartment  $i$ . When a compartmental model is used to represent a biological system, each  
 16 compartment usually represents a part of the body that contains a specific material. For instance,  
 in a very simplified human body representation, the stomach and the blood compartments can  
 18 be defined, as shown in Figure S1. If the material is an oral drug, the first represents the drug  
 concentration into the stomach and the second represents the drug concentration into the blood.  
 20 The two compartments together represent a simplified whole-body model of the drug, starting  
 from the oral intake ( $u(t)$ , the system input), the absorption in the bloodstream (driven by the  
 22 flux  $R_{21}(Q_m^1(t))$ ) and then, finally, the excretion (driven by the excretion rate  $R_{02}(Q_m^2(t))$ ).  
 The fluxes describing the way the drug is absorbed in/or excreted from the blood compartment  
 24 can be represented by any nonlinear or linear relationship, like (S7) or (S8). In the graphical  
 representation of compartmental models, the accessible compartments from outside are denoted



with a dashed line with a bullet. The blood compartment of Figure S1 is denoted as accessible  
2 because of the possibility to measure the drug concentration in the blood of the patient. Moreover,  
if compartment  $i$  is controlled from compartment  $j$ , this action is represented by a dashed arrow.

#### 4 State-Space Representation

Compartmental models can be described with a state-space representation where the quantities of material in each compartment represent the model states. The state-space representation of the model depicted in Figure S1 is

$$\begin{cases} \dot{x}_1(t) = -R_{21}(x_1(t)) + u(t) , \\ \dot{x}_2(t) = R_{21}(x_1(t)) - R_{02}(x_2(t)) , \\ y(t) = \frac{x_2(t)}{V_2} , \end{cases}$$

where  $x_1(t) := Q_m^1(t)$ ,  $x_2(t) := Q_m^2(t)$ ,  $u(t)$  is the system input (oral drug intake),  $y(t)$  is the  
6 system output (drug concentration measured in the blood), and  $V_2$  is the volume of the blood compartment.

8

### References

[S1] C. Cobelli and E. Carson, *Introduction to modeling in physiology and medicine*. Academic  
10 Press, 2008.

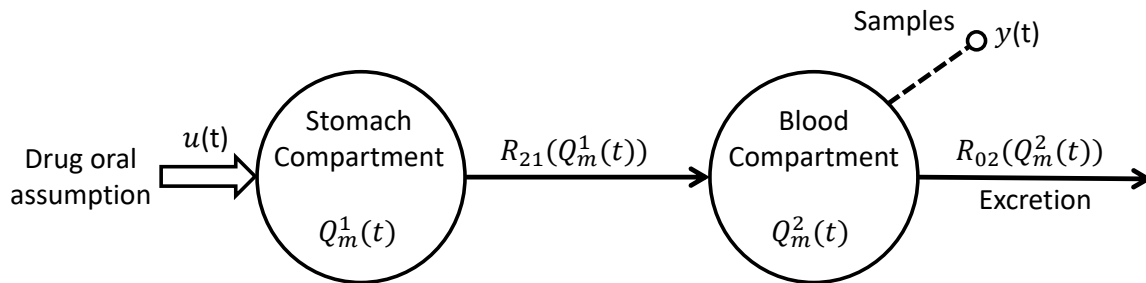


Figure S1. Example of compartmental model with two compartments. The first is the stomach compartment, whereas the second is the blood compartment. The empty arrow represents the drug oral intake  $u(t)$  (system input), the black arrows represent the flow rates, and the dashed line represents the samples  $y(t)$  taken from the blood compartment (system output). The drug quantity in the stomach  $Q_m^1(t)$  is transferred in the blood compartment through the flow rate  $R_{21}(Q_m^1(t))$ . The drug quantity in the blood compartment  $Q_m^2(t)$  is finally excreted through the excretion rate  $R_{02}(Q_m^2(t))$ .

## Author Biography

2 Mirko Messori was born in Castel San Giovanni (PC), Italy, in 1986. He started his first  
job as computer programmer in 2005. In 2007 he began the academic studies and he got his  
4 bachelor graduation in computer engineering with full marks cum laude in 2010 and his master  
graduation in computer engineering, curriculum in automation with full marks cum laude in  
6 2012 at University of Pavia, Italy. In the same year, he was admitted at the PhD School in  
Electronics, Computer Science, and Electrical Engineering at University of Pavia, Italy, and  
8 he got his PhD in January 2016. Mirko Messori is currently collaborating with the artificial  
pancreas research group in Pavia in a post-doctoral position and is working as a freelancer in  
10 machine learning techniques used to predict financial markets.

12 Gian Paolo Incremona was born in Comiso (RG), Italy, in 1988. He received the Master  
Degree (with honor) in Electric Engineering from the University of Pavia, Italy, in 2012. He  
14 was also a student of the Almo Collegio Borromeo of Pavia, and of the class of Science and  
Technology of the Istituto Universitario Studi Superiori (IUSS) of Pavia. Gian Paolo Incremona  
16 got his PhD in Electronics, Electric and Computer Engineering at the University of Pavia in  
2016, where now he is a postdoctoral fellow of the Identification and Control of Dynamic  
18 Systems Laboratory. He works with the artificial pancreas group in Pavia and his research deals  
also with industrial robotics, real-time physical systems, optimal control and variable structure  
20 control methods of sliding mode type.

22 Claudio Cobelli is Full Professor of Biomedical Engineering at University of Padova  
since 1981. From 2000 to 2011 he has been Chairman of the Graduate Program in Biomedical  
24 Engineering and of the PhD Program in Bioengineering at the University of Padova. His  
main research activity is in the field of modeling and identification of physiological systems,  
26 especially the glucose system. His research is currently supported by National Institutes of  
Health (NIH), Juvenile Diabetes Research Foundation International (JDRF) and European  
28 Community. He has published 486 papers in internationally refereed journals, co-author of  
8 books, holds 11 patents, and has an h-index of 88. He is currently Associate Editor of  
30 IEEE Transaction on Biomedical Engineering and Journal of Diabetes Science & Technology.  
He is on the Editorial Board of Diabetes Technology & Therapeutics. Dr. Cobelli has been  
32 Chairman (1999-2004) of the Italian Biomedical Engineering Group, Chairman (1990-1993 &  
1993-1996) of IFAC Technical Committees on Modeling and Control of Biomedical Systems  
34 and member of the IEEE Engineering in Medicine and Biology Society (EMBS) Administrative  
Committee (AdCom) (2008-2009). In 2010 he received the Diabetes Technology Artificial

Pancreas Research Award. He is Fellow of IEEE Biomedical Engineering Society (BMES) and European Alliance for Medical and Biological Engineering & Science (EAMBES).

Lalo Magni is Full Professor of Automatic Control. From October 1996 to February 1997 and in March 1998 he was at Center for Systems Engineering and Applied Mechanics (CESAME), Université Catholique de Louvain, Louvain La Neuve (Belgium). From October to November 1997 he was at the University of Twente with the System and Control Group in the Faculty of Applied Mathematics. He was plenary, semi-plenary or Keynote speaker at the 2nd IFAC Conference “CONTROL SYSTEMS DESIGN” (CSD’03), the Nonlinear Model Predictive Control (NMPC) Workshop on Assessment and Future Direction (2005), the Workshop on Nonlinear Model Predictive Control: Introduction & Current Topics at the 16th IFAC World Congress (2005), the Tutorial on Model Predictive Control at the 18th IFAC World Congress (2011), the IFAC Conference on Nonlinear Model Predictive Control (NMPC12), the IFAC Conference on Nonlinear Model Predictive Control (NMPC15) and the IFAC International Symposium on Advanced Control of Chemical Processes (ADCHEM 2015). His current research interests include nonlinear control, predictive control, receding-horizon control, robust control, process control and artificial pancreas. His research is witnessed by 75 papers published in the main international journals. In 2003, he was Guest Editor of the Special Issue “Control of nonlinear systems with Model Predictive Control” in the International Journal of Robust and Nonlinear Control. He served as an Associate Editor of the IEEE Transactions on Automatic Control and of Automatica. He was subarea Chair for the area “Nonlinear systems optimal and predictive control” at the IFAC Symposium on Nonlinear Control Systems (NOLCOS 2007). He was Chair of the NMPC Workshop on Assessment and Future Direction, September 5-9, 2008 Pavia, Italy. He was the national principal investigator of a Fondo per gli Investimenti della Ricerca di Base (FIRB) project Futuro in Ricerca and the local investigator of an FP7 UE program.